HHS Public Access

Author manuscript

J Bone Miner Res. Author manuscript; available in PMC 2016 May 01.

Published in final edited form as:

J Bone Miner Res. 2015 May ; 30(5): 837–854. doi:10.1002/jbmr.2421.

Netrin-1 Is a Critical Autocrine/Paracrine Factor for Osteoclast Differentiation

Aránzazu Mediero[1], **Bhama Ramkhelawon**[2], **Miguel Perez-Aso**[1], **Kathryn J Moore**[2], and **Bruce N Cronstein**[1]

[1]Division of Translational Medicine, Department of Medicine, NYU School of Medicine, New York, NY, USA

[2]Leon H Charney Division of Cardiology, Department of Medicine, NYU School of Medicine, New York, NY, USA

Abstract

Bone metabolism is a vital process that involves resorption by osteoclasts and formation by osteoblasts, which is closely regulated by immune cells. The neuronal guidance protein Netrin-1 regulates immune cell migration and inflammatory reactions, but its role in bone metabolism is unknown. During osteoclast differentiation, osteoclast precursors increase expression of Netrin-1 and its receptor Unc5b. Netrin-1 binds, in an autocrine and paracrine manner, to Unc5b to promote osteoclast differentiation in vitro, and absence of Netrin-1 or antibody-mediated blockade of Netrin-1 or Unc5b prevents osteoclast differentiation of both murine and human precursors. We confirmed the functional relationship of Netrin-1 in osteoclast differentiation in vivo using Netrin-1-deficient ($Ntn1^{-/-}$) or wild-type (WT) bone marrow transplanted mice. Notably, $Ntn1^{-/-}$ chimeras have markedly diminished osteoclasts, as well as increased cortical and trabecular bone density and volume compared with WT mice. Mechanistic studies revealed that Netrin-1 regulates osteoclast differentiation by altering cytoskeletal assembly. Netrin-1 increases regulator of Rho-GEF subfamily (LARG) and repulsive guidance molecule (RGMa) association with Unc5b, which increases expression and activation of cytoskeletal regulators RhoA and focal adhesion kinase (FAK). Netrin-1 and its receptor Unc5b likely play a role in fusion of osteoclast precursors because Netrin-1 and DC-STAMP are tightly linked. These results identify Netrin-1 as a key regulator of osteoclast differentiation that may be a new target for bone therapies.

Keywords

NETRIN-1; UNC5B; OSTEOCLAST DIFFERENTIATION; RHOA; FAK

Introduction

Osteoclasts, the cells responsible for bone resorption, are large, multinucleated cells derived from hematopoietic stem cells.[1,2] During differentiation, osteoclast precursors express a

Address correspondence to: Bruce N Cronstein, MD, Division of Translational Medicine, Department of Medicine, New York University School of Medicine, 550 First Avenue, MSB251, New York, NY 10016, USA. Bruce.Cronstein@nyumc.org.

Additional Supporting Information may be found in the online version of this article.

number of specific transcriptional regulators, proteases, matrix proteins, cell surface receptors, and other molecules required for bone resorption and fuse to form multinucleated syncytia. A variety of cytokines and other proteins, including members of the family of axonal guidance proteins (eg, semaphorins), which are produced by inflammatory cells, have been shown to regulate osteoclast differentiation.[3]

Netrin-1 is a member of the axonal guidance protein family that is a positive and negative regulator of cell migration both within and outside of the nervous system. This secreted laminin-related protein is a leukocyte-guidance molecule that inhibits migration of monocytes, neutrophils, and lymphocytes by activation of its receptor, Unc5b.[4–6] Netrin-1, acting through Unc5b receptor, reduces renal ischemia–reperfusion injury and its associated renal inflammation,[7] and downregulation of Netrin-1 in vascular endothelial cells promotes endothelial cell activation and infiltration of leukocytes enhancing tubular injury.[8] Netrin-1 is expressed on vascular endothelium, where it is regulated by infection and inflammatory cytokines, and inhibits basal cell migration into tissues, and its downregulation at the onset of sepsis/inflammation may facilitate leukocyte recruitment.[4] Other studies have demonstrated that Netrin-1 promotes chronic inflammation in atherogenesis and diet-induced obesity; tissue macrophages in atherosclerotic plaques and obese adipose tissue increase their expression of Netrin-1,[9,10] which promotes macrophage retention and survival,[11] further increasing chronic inflammation. These in vivo roles of Netrin-1 in regulating inflammation prompted us to investigate its potential function in bone metabolism, which is also highly regulated by inflammatory processes.

Netrin-1 and its receptors, Unc5b and DCC, regulate cellular motility by activating a variety of intracellular pathways. For example, Netrin-1 receptor activation leads to changes in the actin cytoskeleton by regulation of the small GTPases Rac and Rho. Inhibition of Rho promotes axonal outgrowth, whereas inhibition of Rac and CDC42 impairs neurite extension.[12] Netrin-1 also activates the mitogen-activated protein kinase (MAPK) signaling pathway that plays a key role in the regulation of actin-cytoskeleton dynamics during cell motility.[13,14] Recent work has demonstrated that DCC interacts with focal adhesion kinase (FAK), a kinase that has been implicated in the regulation of cell adhesion and migration, and with Src Tyr kinases.[15] In addition, Netrin-1 receptor ligation regulates the intracellular second messengers Ca^{2+}, cyclic AMP (cAMP), and ion channels,[16] which play a role in the attraction and repulsion of axonal growth cones. Finally, Netrin-1 signaling through DCC and Unc5b receptors stimulates cell survival or apoptosis via Unc5b.[17,18]

Based on the recent findings that Netrin-1 regulates the function of myeloid cells and the fact that osteoclasts are derived from myeloid precursors, we investigated whether osteoclasts or other marrow cells expressed Netrin-1 and whether Netrin-1 and its receptors could regulate osteoclast differentiation and/or function. Here we report that Netrin-1, acting via its receptor Unc5b, is an autocrine and paracrine factor that is required for osteoclast differentiation. Moreover, we demonstrate that Netrin-1 binding to Unc5b promotes cytoskeletal assembly, resulting in RhoA activation.

Materials and Methods

Reagents

RAW264.7 cells were from ATCC (Manassas, VA, USA). Human bone marrow cells were purchased from Lonza (Allendale, NJ, USA). Recombinant mouse and human macrophage colony-stimulating factor (M-CSF), receptor activator of NF-κB ligand (RANKL), and Netrin-1 were from R&D Systems (Minneapolis, MN, USA). α-MEM, FBS, penicillin/streptomycin, and Alexa Fluor 555 phalloidin were from Invitrogen (Life Technologies, Carlsbad, CA, USA). Sodium acetate, glacial acetic acid, Naphtol AS MX phosphate disodium salt, Fast Red Violet LB, sodium tartrate, alizarin red, toluidine blue, RIPA buffer, protease inhibitor cocktail, phosphatase inhibitor cocktail, Histopaque 1077, dexamethasone, β-glycerophosphate, L-ascorbic acid, hexadimethrine bromide, lentivirus packaging particles (scrambled, Netrin-1 and Unc5b), puromycin selection marker and goat anti-rabbit-FITC and goat anti-mouse TRITC were from Sigma-Aldrich (St. Louis, MO, USA). Sodium tartrate was from Fisher Scientific (Pittsburgh, PA, USA). Goat polyclonal anti-Netrin-1, rabbit polyclonal anti-Unc5b, mouse monoclonal anti-Unc5b, rabbit polyclonal anti-DCC, rabbit polyclonal anti-FAK, rabbit polyclonal anti-alkaline phosphatase, rabbit polyclonal anti-osteopontin, rabbit polyclonal anti-osteocalcin, and rabbit polyclonal anti-osteonectin were from Abcam (Cambridge, MA, USA). Rabbit anti-pRhoA, mouse anti-RhoA, rabbit polyclonal anti-cathepsin K, rabbit policlonal anti-CD68, rabbit anti-regulator of Rho-GEF subfamily (LARG), rabbit anti-repulsive guidance molecule (RGMa), rabbit anti-Neogenin, and rabbit anti DC-STAMP and mouse monoclonal anti-actin were from Santa Cruz Biotechnology (Dallas, TX, USA). Goat anti-rabbit IRDye 800CW and goat anti-mouse IRDye 680 RD were from Li-cor Biosciences (Lincoln, NE, USA).

Transplantation of fetal liver cells

The NYUSoM Institutional Animal Care and Use Committee approved all protocols related to animals. Female and male *Ntn1*$^{+/-}$ mice were mated. On day 14 of gestation, embryos were dissected free from the placenta and yolk sac, and single-cell suspensions of fetal liver cells were prepared by flushing through graded sizes of needles. A portion of the fetal tissues was used for genotyping by the intensity of 5-bromo-4-chloro-3-indoyl-β-D-galactoside staining; the other portion was used to provide independent confirmation of the genotype by PCR analysis. Fetal liver cells (2×10^6) were injected intravenously into lethally irradiated C57BL/6 mice (two exposures of 600 cGy). Wild-type (WT, Ntn1$^{+/+}$) mice were used as control littermates for fetal liver transplantation.[9] Four weeks after transplantation, in vitro cell differentiation and skeletal analysis were performed.

Confirmation of marrow engraftment

Four to 6 weeks after recovery from transplantation, DNA from mouse blood was isolated with an ArchivePure DNA kit, according to the manufacturer's protocol (5 Prime,). Netrin-1 and B-gal gene expression in blood leukocytes were evaluated by RT-PCR and the percentage of reconstitution was calculated, as previously described. Mice with >95% reconstitution were included in the study.

Transfection protocol

Netrin-1 and Unc5b shRNA transfection was performed as previously described.[19] Briefly, 15000 RAW264.7 cells were plated and 24 hours later cells were incubated in the presence of hexadimethrine bromide (4 μg/mL) and 10^8 lentiviral transduction particles corresponding to mouse Netrin-1 (SHCLNV-NM_008744), Unc5b (SCHLNV-NM_029777), and DC-STAMP (SHCLNV-XM_128030) with puromycin selection marker, for another 24 hours to allow transfection. Media was then replaced with α-MEM containing puromycin (1 μg/mL), changing the media every 3 days until selected clones formed. These clones were isolated and expanded until confluent. Scrambled shRNA (SHC002V) was used as a control. Permanently silenced clones are kept in culture under puromycin selection.

Osteoclast differentiation

After 4 weeks of recovery, the marrow cavity was flushed out with α-MEM from aseptically removed femora and tibias and marrow was incubated overnight in α-MEM containing 10% FBS and 1% penicillin/streptomycin to obtain a single-cell suspension. A total of 200,000 nonadherent cells were collected and seeded in α-MEM with 30 ng/mL M-CSF (R&D) for 2 days. At day 3 (day 0 of differentiation), 30 ng/mL RANKL (R&D) was added to cultures in the presence/absence of recombinant Netrin-1 (250 ng/mL, R&D), Unc5b, or DCC antibodies (200 μg/mL, Abcam) ($n = 6$). Medium and reagents were replaced every third day.

RAW264.7 cells (ATCC; 5000/well) were differentiated with 50 ng/mL RANKL and cultures were treated in the same conditions as described for primary mouse bone marrow cells (BMCs).

Human bone marrow myeloid precursors (Lonza) were separated by density gradient through Histopaque-1077 (Sigma-Aldrich), according to the manufacturer's instructions, and 200,000 cells were seeded in α-MEM with 30 ng/mL M-CSF for 2 days. At day 3 (day 0 of differentiation), 30 ng/mL RANKL was added and cultures were treated as described for primary mouse BMCs. After incubation for 7 (mouse and human BMCs) or 3 days (RAW264.7 cells), cells were stained for tartrate-resistant acid phosphatase (TRAP) for osteoclast quantification as previously described.[20,21] The number of TRAP-positive MNCs containing ≥3 nuclei/cell was scored.[22] To determine whether the effect of Netrin-1 on osteoclast formation varied with exposure time, it was added at 250 ng/mL on consecutive days starting at day 3 and ending 7 days later. In all experiments, DMSO was added to control medium.

To assay resorption activity, 200,000 nonadherent cells were collected and seeded on dentin slides (Immunodiagnostic Systems, Scottsdale, AZ, USA) and were treated in the same conditions as described for TRAP staining. After 7 days of differentiation, resorption was assayed by staining the dentin slides with 1% toluidine blue in 0.5% sodium tetraborate solution following the manufacturer's recommendations. The pits developed blue to purple color.

Osteogenesis assay

Osteogenesis assays were performed as previously described.[23] BMCs were isolated by flushing out the bone marrow cavity from 6- to 8-week-old WT female mice. BMCs were cultured for 3 days, nonadherent cells were discarded and the adherent cells were cultured until confluent. Stromal cells were washed and reseeded in culture dishes at $1*10^5$cell/cm^2 density with osteogenic medium (α-MEM containing 1 μM dexamethasone, 50μg/ml ascorbic acid, and 10mM β-glycerophosphate) in the presence/absence Netrin-1 (250 ng/ml), Unc5b or DCC antibodies (200 μg/ml).

Human bone marrow stromal cells (BMSCs) were isolated by culturing human marrow mononuclear cells for 5 days; adherent BMSCs were seeded at a density of 5×10^4 cells/cm^2 with osteogenic media in the same conditions as described for murine cells. Alizarin red staining was performed 10 days (mouse) and 21 days (human) after culture. Cells were fixed in 4% PFA and stained for 45 minutes with 2% alizarin red.

Morphological characterization of cultured osteoclasts

Osteoclasts were generated from bone marrow cells as described above. A total of 7500 cells/mL were plated on fibronectin-coated glass coverslips under the same conditions as described above. After 7 days in culture, cells were fixed with 4% paraformaldehyde in PBS, blocked with PBS 1% BSA and 0.1% Triton X-100 for 30 minutes, stained fluorescently with Alexa Fluor 555 Phalloidin (Invitrogen, Carlsbad, CA, USA) for 30 minutes, and counterstained with DAPI (Fluoroshield with DAPI mounting media, Sigma-Aldrich) as described previously.[24] To evaluate osteoclast morphology, 400 osteoclasts were examined in each sample using confocal microscopy (Leica SP5 confocal system, Leica Microsystems, Buffalo Grove, IL, USA).

Western blot

Primary mouse or human BMCs were treated with recombinant Netrin-1, Unc5b, or DCC blocking antibodies for either 15 minutes or 24 hours. Cells were lysed with RIPA buffer, and the supernatant contents were extracted with cold ethanol 1% SDS and sonicated. An amount of 4 to 10 μg of protein was subjected to 7.5% or 10% SDS-PAGE and transferred to a nitrocellulose membrane. Nonspecific binding was blocked with TBS/Tween-20 0.05% to 5% skimmed milk. Membranes where incubated overnight (4°C) with primary antibodies against Netrin-1, Unc5b, DCC, pRhoA, RhoA, FAK, and Actin (1:1000 each). Membranes were incubated with goat anti-rabbit IRDye 800CW 1:10,000, donkey anti-goat IRDye 800CV 1:10,000 and goat anti-mouse IRDye 680 RD 1:10,000 (Li-cor Biosciences) in the dark. Proteins were visualized by Li-cor Odyssey equipment, which detects near-infrared fluorescence. As each secondary antibody emits a signal in a different spectrum, reprobing with actin (to check that all lanes were loaded with the same amount of protein) was performed simultaneously with primary antibody incubation. Coomassie blue was used as loading marker for the supernatant proteins. Intensities of the respective band were quantitated by densitometric analysis using Image Studio 2.0.38 software (Li-cor Biosciences). Variations in band intensity were expressed as percentage of unstimulated controls to minimize disparities among different experiments.

Immunoprecipitation

RAW264.7 cells were incubated with RANKL in the presence/absence of recombinant Netrin-1 for 24 hours. An amount of 1000 μg total protein was incubated with 10 μg of affinity-purified Unc5b antibody at 4°C overnight. The immunoprecipitation was performed following the manufacturer's recommendations (Pierce Classic IP kit, ThermoScientific). After gel electrophoresis, membranes were incubated with antibodies to LARG, RGMa, Neogenin, and DC-STAMP (all 1:1000 dilution). To check that all lanes were loaded with the same amount of protein, we also probed the membranes for actin at the same time as the primary antibody incubation.

Immunofluorescence

RAW264.7 cells were transduced with a lentiviral construct expressing shRNA for Netrin-1, Unc5b, DC-STAMP, or a scrambled shRNA as a control. A total of 7500 cells/mL (shRNA) were plated on fibronectin-coated glass coverslips and incubated with 50 ng/mL RANKL for 24 hours. Cells were fixed with 4% paraformaldehyde in PBS. After blocking of nonspecific binding with PBS 3% BSA and 0.1% Triton X-100 for 1 hour, primary antibodies (LARG, RGMa, Neogenin, DC-STAMP, and Unc5b, all 1:200 dilution) were incubated overnight at 4°C in a humidifying chamber. Secondary antibodies goat anti-rabbit-FITC (1:200) and goat anti-mouse TRITC (1:200) were incubated for 1 hour in dark. Slides were mounted with Fluoroshield with DAPI mounting media (Sigma-Aldrich) as described previously.

Gene expression profiling

Total RNA was extracted using RNeasy Mini Kit (Qiagen, Invitrogen) including sample homogenization with QIAshredder columns from both undifferentiated and osteoclast-derived RAW264.7 cells. RNA quality was verified by Pico Chips (5067-1511; Agilent Technologies, Santa Clara, CA, USA). RNA (1 μg) was reverse-transcribed, and quantitative RT-PCR analysis of the Netrin-1 guidance cue family members was performed using RT2 Custom Profiler PCR Arrays (Qiagen), according to the manufacturer's protocol. Data analysis was performed using the manufacturer's integrated web-based software package of the PCR Array System using ΔΔCt-based fold change calculations.

Quantitative real-time RT–PCR

The mRNA expression levels were measured by quantitative RT-PCR (qRT–PCR) as previously described.[19,25] The following primers were used: Netrin-1—Forward: 5'-GCGGGTTATTGAGGTCGGTG-3' and Reverse: 5'-CAGCCTGATCCTTGCTCGG-3'; Unc5b—Forward: 5'-TGGATCTTTCAGCTCAAGACCCAG-3' and Reverse 5'-AAGATGGCCAGCTGGAGCCG-3'; DCC Forward—5'-GCTTTTGTCTCAGCCAGGAC-3' and Reverse: 5'-CGCTCAAGTCATCCTGTTCA-3'; and GAPDH—Forward: 5'-CTACACTGAGGACCAGGTTGTCT-3' and Reverse: 5'-GGTCTGGGATGGAAATTGTG-3'. To validate the effect of Netrin-1 in osteoclast differentiation, we measured the activation of the two osteoclast differentiation markers, cathepsin K and NFATc1, and osteopontin, an extracellular structural protein that initiates the development of osteoclast ruffle borders. LARG, RGMa, and Neogenin expression was also measured. shRNA scrambled and Netrin-1 RAW264.7 cells were collected during the 4

days of differentiation, and mRNA levels were measured by RT-PCR. The following primers were used in real-time PCR amplification: cathepsin K—Forward: 5'-GCTGAACTCAGGACCTCTGG-3' and Reverse: 5'-GAAAAGGGAGGCATGAATGA-3'; NFATc1—Forward: 5'-TCATCCTGTCCAACACCAAA-3' and Reverse: 5'-TCACCCTGGTGTTCTTCCTC-3'; osteopontin—Forward: 5'-TCTGATGAGACCGTCACTGC-3' and Reverse: 5'-TCTCCTGGCTCTCTTTGGAA-3; LARG—Forward 5'-ACACAGTCTACTATCACGGACA-3' and Reverse 5'-AAATCATGCGATGAACTGCGT-3'; RGMa—Forward 5'-CCACACCTCAGGACTTTCACA-3' and Reverse 5'-AGACGGAAGTTCGTCCATTTC-3'; and Neogenin—Forward 5'-TTGCTCGGCATATTCTGAGCC-3' and Reverse 5'-TGGCGTCGATCATCTGATTCTAA-3'. The Pfaffl method[26] was used for relative quantification.

Measurement of bone mineral density (BMD)

We assessed BMD (gm/cm^2) of whole skeletons of 5-month-old mice by PIXImus bone densitometer (Lunar, Madison, WI, USA). The instrument was calibrated before each scanning session, using a phantom with known BMD, according to manufacturer's guidelines. Nine WT and 9 Netrin-$1^{-/-}$ mice were anesthetized by isofluorane inhalational anesthesia and placed in the prone position on the specimen tray for scanning of the entire skeleton.

Micro-X-ray computed tomography (micro-CT) analysis of bone mass

To measure bone volume (trabecular bone volume [BV/TV]), the femurs of 5 WT and 5 Netrin-$1^{-/-}$ mice were measured by micro-CT, as previously described.[20] Analyses were performed in the micro-CT core at the Hospital for Special Surgery using the Scanco Medical MicroCT 35 Scanner (Scanco Medical, Bruttisellen, Switzerland) with 25-μm resolution (KVp: 5T μA/45), and every field of view was scanned by CCD detector, with an integration time of 400 ms. For qualitative analysis, 3D images of the femur were reconstructed from cross-sectional slices using the software provided by Scanco Medical MicroCT 35 and processing was performed to get direct morphometric measurements in 3D.

Histological studies

Mice femurs were fixed in 4% paraformaldehyde and then decalcified in 10% EDTA for 4 weeks. Sections (5 μm) of paraffin-embedded bone were cut and H&E staining was performed.

TRAP staining was carried out with a homemade TRAP buffer (0.1 M acetate buffer, 0.3 M sodium tartrate 10 mg/mL Naphtol AS-MX phosphate, 0.1% Triton X-100, 0.3 mg/mL Fast Red Violet LB). After deparaffinization and acetate buffer washing processes, samples were incubated in TRAP buffer for 30 minutes and counterstained with Fast Green.

Immunohistochemistry analysis of markers for osteoblasts (alkaline phosphatase) and osteoclast (cathepsin K, Santa Cruz Biotechnology) and extracellular matrix proteins (osteopontin, osteonectin, and osteocalcin; Abcam) was carried out as previously described.[27] Deparaffinized and hydrated sections were incubated with Proteinase K

solution (20 μg/mL in TE Buffer, pH 8.0) at 37°C for antigen retrieval. Endogenous peroxidase was removed by incubating sections with 3% H_2O_2 in methanol. Blockade of nonspecific binding was performed with PBS-BSA 3% 1% Triton 5% FBS. Primary antibody (in PBS-BSA 3%) (alkaline phosphatase 1:100, cathepsin K 1:25, osteopontin 1:100, osteocalcin 1:200, osteonectin 1:100) was incubated overnight at 4°C in a humidifying chamber. Secondary goat anti-rabbit HRP antibody (Santa Cruz Biotechnology) was incubated and sections were developed with Fast 3'3'-Diaminobenzidine (Sigma-Aldrich) and counterstained with hematoxylin (Sigma-Aldrich). Slides were mounted using Permount mounting media (Fisher Scientific). Images were observed in a Leica microscope equipped with SlidePath Digital Image Hub Version 3.0 software.

Histomorphometry

Long bones ($n = 4$) were dehydratated with increasing concentration of ethanol and a final step of methyl salicylate incubation for 30 hours, with a change in solution after 6 hours. Tissue was infiltrated with methyl methacrylate, changing the solution every 24 hours 3 times to ensure complete infiltration (first infiltration at room temperature and the other two at 4°C). After this, solution was changed again and samples were kept under UV light until polymerization. The specimen was trimmed of excess polymer and sectioned. Stevenel's blue-Van Geison and TRAP stainings were performed. Digital photographs of the sections were scanned by Aperio (Leica) microscope. Pictures were displayed by Image Scope viewer, which imports a single high-quality, ultra-resolution digital scan that multiple magnified images could be selected from. Using Bioquant Osteo (Nashville, TN, USA) software analysis, a region of interest (ROI) was drawn interactively, for each histologic section. This ROI was subsequently used in all the histomorphometric measurements.

Statistical analysis

Statistical significance for differences between groups was determined by use of one-way ANOVA and Bonferroni post hoc test or Student's *t* test. All statistics were calculated using GraphPad software (GraphPad, La Jolla, CA, USA).

Results

Netrin-1 and its receptor Unc5b expression are increased during osteoclast but not osteoblast differentiation

Because inflammatory cells can coordinate osteoclast differentiation and Netrin-1 has been previously demonstrated to skew inflammatory balance, using a custom array comprising a complete panel of netrin guidance cue and its receptors, we found that Netrin-1 and its chemorepulsive receptor Unc5b mRNA expression were higher in RAW-derived osteoclast than in undifferentiated RAW cells (2.4- and 2.8-fold change, respectively, $p < 0.01$; Fig. 1*A*). These results were confirmed by RT-PCR during osteoblast and osteoclast differentiation in murine BMCs. However, there was no change in expression of Netrin-1, Unc5b, or DCC expression at the mRNA level during osteoblast differentiation (Fig. 1*B*). Netrin-1 and Unc5b mRNA expression increased 2 days after RANKL/M-CSF treatment and were maximally increased coincident with the formation of large TRAP-positive multinucleated cells (13.4-fold change for Netrin-1 and 5.5-fold change for Unc5b receptor

at 7 days, $p < 0.001$ and $p < 0.01$ respectively, $n = 4$ each) (Fig. 1*C*). In contrast, DCC mRNA expression did not change during osteoclast differentiation (Fig. 1*C*).

We next performed Western blots to analyze the protein levels of Netrin-1 and its receptors in differentiated osteoblasts and osteoclasts. Consistent with the unmodified mRNA expressions, osteoblasts did not exhibit any protein expression of Netrin-1, Unc5b, or DCC during their differentiation (Supplemental Fig. S1*A*). Similar results were found in human osteoblast precursors (Supplemental Fig. S2*A*). In contrast, Netrin-1 expression and secretion in the extracellular supernatant of osteoclast precursors were significantly increased when compared with RANKL/M-CSF-untreated cells (130 ± 2% and 166 ± 3% increase, respectively, $p < 0.001$, $n = 4$) (Fig. 2*A*). Similarly, Unc5b receptor expression increased (198 ± 4% increase, $p < 0.001$, $n = 4$), whereas DCC expression did not change during osteoclast differentiation (105 ± 2% of unstimulated expression, p = ns, $n = 4$) (Fig. 2*A*). Similar results were found for human BMCs (Fig. 2*B*).

Netrin-1 and Unc5b are required for osteoclast but not for osteoblast differentiation and function

Because Netrin-1 and Unc5b mRNA and protein levels were upregulated in osteoclast, we determined their functional significance during this process in primary murine bone marrow cells in vitro. Although the treatment of WT BMCs with recombinant Netrin-1 increased the number of TRAP-positive multinucleated cells (115 ± 5% of control with RANKL alone, $p < 0.5$, $n = 6$) (Fig. 3*A*), the addition of a blocking antibody against the Unc5b receptor markedly reduced the number of TRAP-positive osteoclasts (43 ± 4% of control with RANKL alone, $p < 0.001$, $n = 6$). This effect was specific to the Unc5b receptor because the addition of a blocking antibody to DCC did not affect osteoclast differentiation in vitro (94 ± 2% of control with RANKL alone, p = ns, $n = 4$) (Fig. 3*A*). Interestingly, osteoclast differentiation by bone marrow precursors that did not express Netrin-1 was markedly reduced compared with wild-type precursors when studied in vitro (44 ± 4% of WT cells, $p < 0.001$, $n = 6$) (Fig. 3*A*), which was normalized by addition of recombinant Netrin-1 (122 ± 5% of control in WT cells, $p < 0.5$, $n = 6$). Under these conditions, blocking the Unc5b receptor, but not the DCC receptor, inhibited osteoclast differentiation in the presence of exogenous Netrin-1 (Unc5b blocking Ab, 46 ± 4% of control in WT cells, $p < 0.001$; DCC blocking Ab, 95 ± 5% of control in WT cells, $p < 0.001$, $n = 6$; Fig. 3*A*). These data strongly suggested an important role of Netrin-1/Unc5b interactions in osteoclast differentiation.

To determine whether Netrin-1 was also required for osteoclast function, we determined whether antibodies to Netrin-1 or Unc5b affected bone resorption in vitro. Morphometric measurement of toluidine blue-stained dentin clearly demonstrated a marked reduction in pit formation when osteoclasts were differentiated in the presence of antibodies to either Netrin-1 or Unc5b but not to DCC (Fig. 3*B*). These results mirrored the effects of Netrin-1 or anti-Unc5b on osteoclast differentiation in vitro, as described above.

To define the stage of osteoclast formation and function affected by Netrin-1 stimulation, we treated BMC cultures with antibodies to Netrin-1, Unc5b, or DCC at various time points after initiation of osteoclast differentiation. Antibodies to Netrin-1 or Unc5b blocked osteoclast differentiation only when added during the first 4 days of culture (Fig. 3*C*).

Antibody-mediated blockade of Unc5b completely blocked osteoclast differentiation despite treatment with exogenous Netrin-1 (Fig. 3*C*), but antibodies to DCC did not affect osteoclast differentiation when added or removed at any time point.

Because factors required for murine osteoclast formation may differ from those required for human osteoclast differentiation, we determined whether recombinant Netrin-1 affects differentiation of osteoclasts and osteoblasts from primary human bone marrow-derived osteoclasts and osteoblasts. Addition of recombinant Netrin-1 increased the number of TRAP-positive cells when compared with RANKL alone (Fig. 3*D*), which was reversed by addition of antibody to Unc5b receptor but not by anti-DCC antibody (Fig. 3*D*), suggesting that this mechanism holds true in human osteoclast differentiation and function.

To further confirm the involvement of Netrin-1 and Unc5b receptors in osteoclast differentiation, RAW264.7 cells were transduced with a lentiviral construct expressing shRNA for Netrin-1 or Unc5b or a scrambled shRNA as a control.[19] When RAW264.7 cells were infected with scrambled shRNA, recombinant Netrin-1 treatment promoted osteoclast differentiation and pretreatment with antibody to Unc5b inhibited osteoclast differentiation (Fig. 3*E*). When Netrin-1 was permanently knocked down by a lentiviral-delivery Netrin-1 shRNA, no osteoclast differentiation was observed, but recombinant Netrin-1 treatment promoted osteoclast differentiation (Fig. 3*E*) and pretreatment with antibody to Unc5b inhibited osteoclast differentiation. When Unc5b was permanently knocked down by lentiviral-delivery of Unc5b shRNA, we observed that neither RANKL alone nor RANKL plus recombinant Netrin-1 induced osteoclast differentiation (Fig. 3*E*). This result provides further supporting evidence that Netrin-1, acting through Unc5b, is a critical factor in osteoclast differentiation.

To confirm that Netrin-1 is a key factor in osteoclast differentiation, we determined the expression of mRNA for markers of osteoclast differentiation in RAW264.7 cells transfected with shRNA for Netrin-1. As shown in Fig. 3*F*, treatment of RAW264.7 cells infected with scrambled shRNA with 50 ng/mL RANKL increased the expression of mRNA for cathepsin K (by up to 3 ± 0.7-fold change on day 4; $p < 0.05$, $n = 4$), an effect that was abrogated in Netrin-1 shRNA-expressing cells. The same effect was found for NFATc1 mRNA expression: RANKL increased NFATc1 mRNA expression by 3.5 ± 0.4-fold on day 4 of differentiation ($p < 0.05$; $n = 4$, Fig. 3*F*), and this upregulation was lost when Netrin-1 was knocked down. Finally, mRNA expression for osteopontin was also increased in the RANKL-stimulated RAW264.7 cells (scrambled shRNA-transduced cells) by up to 2 ± 0.4-fold change on day 2 ($p < 0.001$, $n = 4$), and knockdown of Netrin-1 significantly prevented the RANKL-mediated increase in mRNA levels (Fig. 3*F*).

Alizarin red staining of osteoblast cultures (Supplemental Fig. S1*B*) demonstrated that neither addition of recombinant Netrin-1 nor antibodies to Netrin-1, Unc5b, or DCC affected formation of mineralized bone nodules by differentiated osteoblasts when compared with untreated controls. Similar results were observed in human osteoblast precursors (Supplemental Fig. S2*B*).

Histomorphometric analysis of Netrin-1$^{-/-}$ skeletons reveals increased bone mass

Because both Netrin-1 and Unc5b were upregulated during osteoclast differentiation, we postulated that Netrin-1$^{-/-}$ mice may have a bone phenotype. We examined the skeletons of Netrin-1$^{-/-}$ chimeric mice (Netrin-1$^{-/-}$), in which only bone marrow–derived cells lack expression of Netrin-1 and compared them with mice transplanted with WT bone marrow using whole-body dual X-ray absorptiometry (DXA) scanning. We found a marked increase in bone mineral density (BMD) in the Netrin-1$^{-/-}$ chimeric mice when compared with WT animals (Fig. 4*A*). These results were confirmed by micro-CT analysis of femurs, which revealed a significant increase in total volume (TV), bone volume (BV), and bone volume/total volume ratio (BV/TV) in both cortical and trabecular bone of Netrin-1$^{-/-}$ mice as compared with WT mice (Fig. 4*B*, *C*).

Histologic examination indicated that there were fewer TRAP-positive osteoclasts in the femoral metaphysis of Netrin-1$^{-/-}$ bone marrow chimeric mice than in WT bone marrow chimeric mice (Fig. 5). Similar results were obtained when osteoclasts were identified by immunohistologic staining for cathepsin K. In contrast, there was no change in the number of alkaline phosphatase–positive osteoblasts on bone-forming surfaces, suggesting that the increase in bone density and volume resulted from diminished bone resorption in the Netrin-1$^{-/-}$ chimeric mice. Osteopontin (a matrix protein that initiates development of osteoclasts' ruffled borders) colocalized with osteoclasts on the surface of bone. In contrast, expression of osteonectin (a Ca^{++}-binding glycoprotein secreted by osteoblasts during bone formation) or osteocalcin (a protein secreted by osteoblasts) was similar in WT and Netrin-1$^{-/-}$ chimeric mice (Fig. 5).

To fully describe the cellular changes that lead to increased bone in Netrin-1$^{-/-}$ bone marrow chimeric mice, complete histomorphometric analysis in methyl methacrylate–embedded samples was performed. Using Bioquant Osteo software, changes in BV, TV, BV/TV, trabecular number, trabecular separation, osteoid number, osteoblast number, osteoclast number, as well as number of cells per surface were calculated (Table 1). Histomorphometry analysis confirmed our micro-CT and histology results, showing a significant increase in TV, BV, BV/TV, and a decrease in osteoclast number (Oc.N) and surface (Oc.N/BS) in Netrin-1$^{-/-}$ mice compared with WT mice (Table 1). We have also observed an increase in trabecular number (Tb.N), trabecular separation (Tb.Sp, μm), and osteoid number (OS) and surface (OS/BS) when compared with WT mice (Table 1). In the case of osteoblast number (Ob.N) and surface (Ob.N/S), in Netrin-1$^{-/-}$ mice there is a small but significant increase in number compared with WT mice (Table 1). These results provide further evidence of an uncoupling between osteoclast and osteoblast differentiation and function in Netrin-1$^{-/-}$ mice.

Stimulation of Unc5b promotes cytoskeletal changes associated with osteoclast maturation

Our results indicate that Netrin-1, acting through Unc5b, is an essential autocrine factor for osteoclast differentiation. To gain insight into the mechanism by which Netrin-1, acting through Unc5b, regulates osteoclast maturation and morphology, we examined cytoskeletal changes associated with osteoclast maturation upon netrin-1 stimulation. Osteoclasts

cultured on glass show evidence of three distinct morphologies:[21] least mature osteoclasts (small with centrally located nuclei surrounded by a ring of F-actin and an absence of podosomes); an intermediate stage of maturing osteoclasts (variable in size, dendritic shaped, that contain >5 nuclei with podosomes in patches connected with other maturing cells through cytoplasmic bridges); and the late stage of mature osteoclasts (large multinucleated with a peripheral podosome belt, Fig. 6*A*). Netrin-1 stimulated a marked increase in the number of mature osteoclasts (Fig. 6*B*) similar to classical osteoclast differentiation factors such as M-CSF/RANKL. Differentiation into mature osteoclasts was almost completely blocked by pretreatment with Unc5b blocking antibody but not by DCC antibody (Fig. 6*B*).

Because the chemorepulsant Netrin-1 regulates cytoskeletal assembly, which is critical for osteoclast differentiation, we determined whether Netrin-1, acting via Unc5b, regulated small GTPases, such as RhoA, and focal adhesion kinase (FAK) family kinases, key modulators in osteoclast morphology and function.[28] As previously reported, treatment of osteoclast precursors with RANKL leads to RhoA phosphorylation (170 ± 8% of control phospho-RhoA, $p < 0.01$, $n = 4$), an effect modestly, but not significantly, increased by treatment with recombinant Netrin-1 (Fig. 7*A*, 181 ± 15% of resting, $p < 0.001$ versus control, $n = 4$). As with the effects on osteoclast differentiation, antibody-mediated blockade of Unc5b completely abrogated the effect of Netrin-1 and RANKL on RhoA phosphorylation (93 ± 3% of resting, p = ns versus control, $n = 4$), whereas pre-incubation with an antibody to DCC did not affect RANKL-induced RhoA phosphorylation (182 ± 12% of control, p = ns versus control, $n = 4$) (Fig. 7*A*). The effects of Netrin-1, acting via Unc5b, on FAK expression paralleled the effects on RhoA activation. RANKL stimulated a rapid increase in FAK expression (143 ± 6% of control expression, $p < 0.01$ versus unstimulated, $n = 4$), which was unaffected by Netrin-1 (148 ± 4% of control, $p < 0.01$, $n = 4$) (Fig. 7*B*). As with RhoA phosphorylation, pretreatment with Unc5b antibody completely blocked the increase in FAK expression (97 ± 4% of control, p = ns, $n = 4$), whereas pretreatment with DCC antibody had no effect on FAK expression (126 ± 13% of control, $p < 0.01$, $n = 4$) (Fig. 7*B*). Knockdown of Unc5b in RAW264.7 cells abrogated RANKL- and Netrin-1-stimulated RhoA activation and increased FAK expression (Supplemental Fig. S3). Neither Netrin-1 treatment nor Unc5b blockade or knockdown affected cdc42 or Rac1 expression in either primary murine bone marrow cells or RANKL-treated RAW264.7 cells (data not shown).

To better understand how RhoA and FAK were activated by Netrin-1, we determined whether proteins previously shown to regulate cytoskeletal activation in neuronal cells treated with Netrin-1, LARG, and RGMa associated with Unc5b in osteoclasts. When we added Netrin-1 to osteoclast precursors, we found that Unc5b expression was increased, as shown in Fig. 7*C*, and there was an increase in the amount of LARG and RGMa, which co-precipitated with Unc5b. In contrast, Netrin-1 treatment did not increase the amount of Neogenin, another protein previously reported to associate with Netrin-1, which co-precipitated with Unc5b. In addition, mRNA levels for LARG, RGMA, and Neogenin were increased by 50 ng/mL RANKL 24 hours after stimulation, and these increases were abrogated when Netrin-1 was knocked down (Fig. 7*D*). Moreover, the basal level was lower

in Netrin-1 shRNA cells when compared with scrambled shRNA-infected RAW264.7 cells. Double immunostaining for LARG, RGMa, or Neogenin (green) and Unc5b (red) revealed a colocalization of these proteins in RAW264.7 cells infected with scrambled shRNA cells after 24 hours 50 ng/mL RANKL treatment (Figs. 9–11). Knockdown of Netrin-1 and Unc5b produced a decrease in signal for all of them (Figs. 9–11).

These findings suggest that Netrin-1 ligates and activates Unc5b, which increases recruitment of LARG and RGMa to the Unc5b/Neogenin complex. FAK, interacting with LARG, activates RGMa, which increases RhoA activation, resulting in the osteoclast cytoskeleton rearrangements required for differentiation (Fig. 7*E*).

Unc5b is linked to expression of DC-STAMP

As described in Fig. 3*C*, Netrin-1 or Unc5b needs to be active from the beginning of the osteoclast differentiation process to have an effect. This indicates that Netrin-1 and Unc5b may be important for cell fusion. To test this hypothesis, we studied if there were changes in DC-STAMP (dendritic cell–specific transmembrane protein, a molecule required for osteoclast fusion[29]) expression when Netrin-1 was added to osteoclast precursors. We found that DC-STAMP co-precipitated with Unc5b (Fig. 8*A*). Immunostaining revealed colocalization of DC-STAMP (red) with Unc5b (green) (Fig. 8*B*) that was abrogated when Unc5b was knocked down but not when Netrin-1 was absent (Fig. 8*B*). Moreover, when DC-STAMP was knocked down, Unc5b was not expressed (Fig. 8*B*).

When LARG, RGMa, and Neogenin immunolocalization was studied in DC-STAMP shRNA cells, we found that LARG expression was almost absent (Fig. 9), whereas RGMa and Neogenin were present in cells 24 hours after RANKL incubation but at lower levels when compared with scrambled shRNA-infected cells (Figs. 10 and 11).

Discussion

We provide the first evidence that the neuro-immune protein Netrin-1 is an autocrine and paracrine regulator of osteoclast differentiation. The significance of this finding is underlined by the observation that mice that have undergone bone marrow transplantation with Netrin-1$^{-/-}$ marrow demonstrate a marked increase in bone density after as little as 6 weeks. Moreover, we report here that Netrin-1 mediates its effects on osteoclast precursors via its receptor Unc5b. The binding of Netrin-1 to Unc5b triggers the signaling cascade involved in the activation of the small GTPase RhoA by a mechanism that has not previously been observed in osteoclast precursors. Activation of RhoA via LARG and RGMa leads to the cytoskeletal rearrangements required for osteoclast differentiation.

A number of factors regulate bone metabolism, and there is growing appreciation that axonal guidance proteins and neurotrophins produced by a variety of cells in or near bone play a role in regulating the function and differentiation of the cells involved in bone remodeling. Mammalian bone is innervated by sympathetic and sensory nerves, which are particularly abundant in regions of high bone formation and remodeling, such as the growth plate.[30,31] Togari and colleagues described the expression of mRNA for axonal guidance proteins, including Semaphorins, Netrins, and neurotrophins, in human osteoblast cell lines,

osteosarcoma cell lines, and osteoclasts.[32] Since that initial description, others have demonstrated that Semaphorins and Ephrins play important roles in regulating bone cell differentiation and activity.[33–37] Semaphorin 4D, secreted by osteoclasts, binds to its receptor Plexin-B1 on osteoblasts, resulting in the activation and autophosphorylation of ErbB2, RhoA-ROCK activation, and forward inhibition of IRS-1, thereby diminishing osteoblast differentiation induced by RhoA activation.[34,37] Semaphorin 3A, produced by osteoblasts among other cells, binds to its receptor Neuropilin-1 to both inhibit RANKL-induced osteoclast differentiation and to stimulate osteoblast differentiation and function.[36] Eph/ephrin interactions also regulate both osteoclast and osteoblast differentiation and function.[38] BDNF stimulates osteoclastogenesis and has been reported to mediate, at least in part, the bone destruction that occurs in patients with multiple myeloma.[39,40] Slit proteins, acting through their receptors Robo1/2, have been reported to inhibit osteoblast differentiation and function.[41] Finally, anti-NGF antibodies are undergoing testing in the clinic for the treatment of osteoarthritis and back pain, and one of the toxicities that has been well described is osteonecrosis of bone, although the mechanism for this toxicity has not been defined to date[42] and the effects of NGF (or NGF blockade) on bone metabolism have not been reported. Thus, although axonal guidance proteins and neurotrophins have been described to participate in bone remodeling, we hereby describe the unique role of Netrin-1 that acts both in an autocrine and a paracrine manner to synchronize osteoclast differentiation.

The increase in bone mineral density and bone volume observed in the mice transplanted with Netrin-1-deficient marrow is consistent with the near complete absence of osteoclasts and the slight increase in osteoblast number that we observed. As noted above, osteoclasts secrete products that inhibit osteoblast differentiation and function (eg, semaphorin 4D) and diminished osteoclast function and number might lead to fewer suppressive signals for osteoblasts. However, we did not observe any direct effect of Netrin-1 on bone formation in an in vitro bone formation model. Although prior work indicates that only hematopoietic stem cells are of donor origin in bone marrow chimeras,[43–45] recent work suggests that mesenchymal stem cells (precursors to osteoblasts) are also of donor origin.[46] Nonetheless, the only cells that appear to express Netrin-1 in bone marrow are osteoclasts and a few CD68-positive monocyte/macrophages and in the absence of any demonstrable increase in osteoblast number the absence of osteoclasts alone is sufficient to explain the observed changes in bone mass.

We observed that treatment in vitro with antibodies to either Netrin-1 or Unc5b blocks osteoclast differentiation when added during the first four days of osteoclast differentiation but not after that time, suggesting that the effects of Netrin-1 are mediated early in the process of osteoclast differentiation. We have demonstrated Netrin-1-Unc5b-mediated cytoskeletal changes in osteoclast precursors, and it is possible that the effects of Netrin-1 on cytoskeletal rearrangement are permissive with respect to later events in osteoclast differentiation such as cellular fusion, expression of osteoclast-specific genes, or interaction with components of the bone matrix.

In this work, we have found that Netrin-1 stimulates changes in the osteoclast cytoskeleton by activation of RhoA and FAK (Fig. 7*D*). As previously noted, osteoclasts have a unique

cytoskeleton that plays a critical role in the resorptive process, and this is one of the distinctive characteristics of osteoclasts.[28,47] Previous results have shown that regulation of the small GTPases Rac and Rho allows cell motility via activation by Netrin-1, and inhibition of Rho promotes axon outgrowth, whereas inhibition of Rac and CDC42 impairs neurite extension.[12] We found that the stimulation of the Unc5b receptor by Netrin-1 activates RhoA, leading to cytoskeletal rearrangements required for osteoclast formation (Fig. 7*D*). In parallel, the blockade of Unc5b inhibits RhoA and FAK activation that hinders cytoskeletal organization during osteoclast differentiation. This effect seems to be specific for the Unc5b receptor because the inactivation of the DCC receptor did not modulate Netrin-1-induced osteoclast differentiation. Interestingly, although in other cell systems, DCC receptor stimulation has also been shown to activate FAK,[15] its distinct role from Unc5b in osteoclast differentiation is demonstrated herein. As described above, once osteoclast precursors are activated with RANKL, the presence of Netrin-1 activates the Unc5b receptor, which is associated with Neogenin allowing the recruitment of RGMa. By interaction with FAK, LARG activates RGMa and thereby increases RhoA activation (Fig. 7*D*). Interestingly, neither LARG nor RGMa have previously been shown to play a role in osteoclast differentiation but have only been described in mediating Unc5B-dependent recruitment of Neogenin as a co-receptor and LARG as an effector in neurons.[48]

As described, fusion of osteoclast precursors is a critical event in osteoclast differentiation and DC-STAMP expression, a seven-transmembrane protein originally identified in dendritic cells, is critical for fusion and differentiation of osteoclasts.[29] We found that in the presence of Netrin-1, DC-STAMP co-precipitated with Unc5b receptor and immunostaining revealed colocalization of DC-STAMP and Unc5b in cells, which was abrogated when Unc5b was knocked down but not when Netrin-1 was absent. This finding is consistent with the notion that Netrin-1-Unc5b ligand-receptor interactions and downstream cytoskeletal alterations are important for cell fusion. Nonetheless, fusion is not the only event regulated by Netrin-1 because in the absence of Netrin-1, there is reduced expression of NFATc1, cathepsin K, and osteopontin after RANKL stimulation of osteoclast precursors.

Because of its chemorepulsant activities, Netrin-1 has been reported to be anti-inflammatory in a number of settings, including inflammatory bowel disease, pancreatitis, peritonitis, and pulmonary inflammation.[4,5,7,8,49–54] In contrast, Netrin-1 plays a critical role in promoting atherogenesis by inhibiting macrophage emigration from plaque.[9,11] Because increased bone resorption is a common manifestation of inflammatory bone disease, such as rheumatoid arthritis, it is likely that Netrin-1, produced by osteoclasts or stimulated macrophages, plays a role in inflammatory osteolysis by enhancing osteoclast differentiation.

In conclusion, our results indicate that Netrin-1 is an autocrine and paracrine factor produced by osteoclast precursors and inflammatory cells that enhances osteoclast differentiation and function. Netrin-1 binds to its receptor, Unc5b, and this interaction is required for osteoclast differentiation and function both in vitro and in vivo. Thus, Netrin-1 may be a novel therapeutic target for the reduction of osteoclast-mediated bone resorption and other forms of inflammatory bone destruction.

Supplementary Material

Refer to Web version on PubMed Central for supplementary material.

Acknowledgments

This work was supported by grants from the National Institutes of Health (AR56672, AR54897, AR046121, RC1HL100815), the NYU-HHC Clinical and Translational Science Institute (UL1TR000038), the NYUCI Center Support Grant, 9NIH/NCI 5 P30CA16087-310, and grants from Celgene, AstraZeneca, and Gilead Pharmaceuticals.

Disclosures

AM and BNC have filed a patent on use of adenosine $A_{2A}R$ agonists to prevent prosthesis loosening (pending). AM, BNC, BR, and KJM have filed a patent on use of anti-netrin-1 antibodies for the treatment of bone disease (pending). MP-A does not have any disclosures. BNC holds patent numbers 5,932,558; 6,020,321; 6,555,545; 7,795,427; adenosine A_1R and $A_{2B}R$ antagonists to treat fatty liver (pending); adenosine $A_{2A}R$ agonists to prevent prosthesis loosening (pending). BNC is a consultant for Bristol-Myers Squibb, Novartis, Eli Lilly & Co., CanFite Biopharmaceuticals, Cypress Laboratories, Regeneron (Westat, DSMB), Endocyte, Protalex, Allos, Inc., Savient, Gismo Therapeutics, Antares Pharmaceutical, Medivector, King Pharmaceutical, Celizome, Tap Pharmaceuticals, Prometheus Laboratories, Sepracor, Amgen, Combinatorx, Kyowa Hakka, Hoffman-LaRoche and Avidimer Therapeutics. BNC has stock in CanFite Biopharmaceuticals.

References

1. Suda T, et al. Modulation of osteoclast differentiation and function by the new members of the tumor necrosis factor receptor and ligand families. Endocr Rev. 1999; 20(3):345–357. [PubMed: 10368775]
2. Manolagas SC. Birth and death of bone cells: basic regulatory mechanisms and implications for the pathogenesis and treatment of osteoporosis. Endocr Rev. 2000; 21(2):115–137. [PubMed: 10782361]
3. Boyce BF. Advances in the regulation of osteoclasts and osteoclast functions. J Dent Res. 2013; 92(10):860–867. [PubMed: 23906603]
4. Ly NP, et al. Netrin-1 inhibits leukocyte migration in vitro and in vivo. Proc Natl Acad Sci USA. 2005; 102(41):14729–14734. [PubMed: 16203981]
5. Mirakaj V, et al. Netrin-1 dampens pulmonary inflammation during acute lung injury. Am J Respir Crit Care Med. 2010; 181(8):815–824. [PubMed: 20075388]
6. Rosenberger P, et al. Hypoxia-inducible factor-dependent induction of netrin-1 dampens inflammation caused by hypoxia. Nat Immunol. 2009; 10(2):195–202. [PubMed: 19122655]
7. Tadagavadi RK, Wang W, Ramesh G. Netrin-1 regulates Th1/Th2/Th17 cytokine production and inflammation through UNC5B receptor and protects kidney against ischemia-reperfusion injury. J Immunol. 2010; 185(6):3750–3758. [PubMed: 20693423]
8. Wang W, Reeves WB, Ramesh G. Netrin-1 and kidney injury. I. Netrin-1 protects against ischemia-reperfusion injury of the kidney. Am J Physiol Renal Physiol. 2008; 294(4):F739–F747. [PubMed: 18216145]
9. van Gils JM, et al. The neuroimmune guidance cue netrin-1 promotes atherosclerosis by inhibiting the emigration of macrophages from plaques. Nat Immunol. 2012; 13(2):136–143. [PubMed: 22231519]
10. Ramkhelawon B, et al. Netrin-1 promotes adipose tissue macrophage retention and insulin resistance in obesity. Nat Med. 2014; 20(4):377–384. [PubMed: 24584118]
11. Ramkhelawon B, et al. Hypoxia induces netrin-1 and Unc5b in atherosclerotic plaques: mechanism for macrophage retention and survival. Arterioscler Thromb Vasc Biol. 2013; 33(6):1180–1188. [PubMed: 23599441]
12. Causeret F, et al. Distinct roles of Rac1/Cdc42 and Rho/Rock for axon outgrowth and nucleokinesis of precerebellar neurons toward netrin 1. Development. 2004; 131(12):2841–2852. [PubMed: 15151987]

13. Giancotti FG, Ruoslahti E. Integrin signaling. Science. 1999; 285(5430):1028–1032. [PubMed: 10446041]
14. Forcet C, et al. Netrin-1-mediated axon outgrowth requires deleted in colorectal cancer-dependent MAPK activation. Nature. 2002; 417(6887):443–447. [PubMed: 11986622]
15. Li W, et al. Activation of FAK and Src are receptor-proximal events required for netrin signaling. Nat Neurosci. 2004; 7(11):1213–1221. [PubMed: 15494734]
16. Nishiyama M, et al. Cyclic AMP/GMP-dependent modulation of Ca2+ channels sets the polarity of nerve growth-cone turning. Nature. 2003; 423(6943):990–995. [PubMed: 12827203]
17. Tanikawa C, et al. p53RDL1 regulates p53-dependent apoptosis. Nat Cell Biol. 2003; 5(3):216–223. [PubMed: 12598906]
18. Mehlen P, Furne C. Netrin-1: when a neuronal guidance cue turns out to be a regulator of tumorigenesis. Cell Mol Life Sci. 2005; 62(22):2599–2616. [PubMed: 16158190]
19. Mediero A, Perez-Aso M, Cronstein BN. Activation of adenosine A2A receptor reduces osteoclast formation via PKA- and ERK1/2-mediated suppression of NFkappaB nuclear translocation. Br J Pharmacol. 2013; 169(6):1372–1388. [PubMed: 23647065]
20. Mediero A, et al. Adenosine A2A receptor activation prevents wear particle-induced osteolysis. Sci Transl Med. 2012; 4(135):135ra65.
21. Mediero A, et al. Adenosine A(2A) receptor ligation inhibits osteoclast formation. Am J Pathol. 2012; 180(2):775–786. [PubMed: 22138579]
22. Yasuda H, et al. A novel molecular mechanism modulating osteoclast differentiation and function. Bone. 1999; 25(1):109–113. [PubMed: 10423033]
23. He W, et al. Adenosine regulates bone metabolism via A1, A2A, and A2B receptors in bone marrow cells from normal humans and patients with multiple myeloma. FASEB J. 2013; 27(9):3446–3454. [PubMed: 23682121]
24. Chitu V, et al. The PCH family member MAYP/PSTPIP2 directly regulates F-actin bundling and enhances filopodia formation and motility in macrophages. Mol Biol Cell. 2005; 16(6):2947–2959. [PubMed: 15788569]
25. Mediero A, et al. Adenosine A(2A) receptor ligation inhibits osteoclast formation. Am J Pathol. 2012; 180(2):775–786. [PubMed: 22138579]
26. Pfaffl MW. A new mathematical model for relative quantification in real-time RT-PCR. Nucleic Acids Res. 2001; 29(9):e45. [PubMed: 11328886]
27. Mediero A, et al. Adenosine A2A receptor activation prevents wear particle-induced osteolysis. Sci Transl Med. 2012; 4(135):135ra65.
28. Shahrara S, et al. Differential expression of the FAK family kinases in rheumatoid arthritis and osteoarthritis synovial tissues. Arthritis Res Ther. 2007; 9(5):R112. [PubMed: 17963503]
29. Yagi M, et al. DC-STAMP is essential for cell-cell fusion in osteoclasts and foreign body giant cells. J Exp Med. 2005; 202(3):345–351. [PubMed: 16061724]
30. Bjurholm A. Neuroendocrine peptides in bone. Int Orthop. 1991; 15(4):325–329. [PubMed: 1725676]
31. Hohmann EL, et al. Innervation of periosteum and bone by sympathetic vasoactive intestinal peptide-containing nerve fibers. Science. 1986; 232(4752):868–871. [PubMed: 3518059]
32. Togari A, et al. Expression of mRNA for axon guidance molecules, such as semaphorin-III, netrins and neurotrophins, in human osteoblasts and osteoclasts. Brain Res. 2000; 878(1–2):204–209. [PubMed: 10996153]
33. Edwards CM, Mundy GR. Eph receptors and ephrin signaling pathways: a role in bone homeostasis. Int J Med Sci. 2008; 5(5):263–272. [PubMed: 18797510]
34. Kang S, Kumanogoh A. Semaphorins in bone development, homeostasis, and disease. Semin Cell Dev Biol. 2013; 24(3):163–171. [PubMed: 23022498]
35. Fukuda T, et al. Sema3A regulates bone-mass accrual through sensory innervations. Nature. 2013; 497(7450):490–493. [PubMed: 23644455]
36. Hayashi M, et al. Osteoprotection by semaphorin 3A. Nature. 2012; 485(7396):69–74. [PubMed: 22522930]

37. Negishi-Koga T, et al. Suppression of bone formation by osteoclastic expression of semaphorin 4D. Nat Med. 2011; 17(11):1473–1480. [PubMed: 22019888]
38. Sims NA, Walsh NC. Intercellular cross-talk among bone cells: new factors and pathways. Curr Osteoporos Rep. 2012; 10(2):109–117. [PubMed: 22427140]
39. Ai LS, et al. Inhibition of BDNF in multiple myeloma blocks osteoclastogenesis via down-regulated stroma-derived RANKL expression both in vitro and in vivo. PLoS One. 2012; 7(10):e46287. [PubMed: 23077504]
40. Sun CY, et al. Brain-derived neurotrophic factor is a potential osteoclast stimulating factor in multiple myeloma. Int J Cancer. 2012; 130(4):827–836. [PubMed: 21400510]
41. Sun H, et al. Regulation of osteoblast differentiation by slit2 in osteoblastic cells. Cells Tissues Organs. 2009; 190(2):69–80. [PubMed: 19033678]
42. Halvorson KG, et al. A blocking antibody to nerve growth factor attenuates skeletal pain induced by prostate tumor cells growing in bone. Cancer Res. 2005; 65(20):9426–9435. [PubMed: 16230406]
43. Simmons PJ, et al. Host origin of marrow stromal cells following allogeneic bone marrow transplantation. Nature. 1987; 328(6129):429–432. [PubMed: 2886914]
44. Koc ON, et al. Bone marrow-derived mesenchymal stem cells remain host-derived despite successful hematopoietic engraftment after allogeneic transplantation in patients with lysosomal and peroxisomal storage diseases. Exp Hematol. 1999; 27(11):1675–1681. [PubMed: 10560915]
45. Awaya N, et al. Failure of adult marrow-derived stem cells to generate marrow stroma after successful hematopoietic stem cell transplantation. Exp Hematol. 2002; 30(8):937–942. [PubMed: 12160845]
46. Reyes M, et al. Donor origin of multipotent adult progenitor cells in radiation chimeras. Blood. 2005; 106(10):3646–3649. [PubMed: 16099880]
47. Ross FP, Teitelbaum SL. alphavbeta3 and macrophage colony-stimulating factor: partners in osteoclast biology. Immunol Rev. 2005; 208:88–105. [PubMed: 16313343]
48. Hata K, et al. Unc5B associates with LARG to mediate the action of repulsive guidance molecule. J Cell Biol. 2009; 184(5):737–750. [PubMed: 19273616]
49. Aherne CM, et al. Neuronal guidance molecule netrin-1 attenuates inflammatory cell trafficking during acute experimental colitis. Gut. 2012; 61(5):695–705. [PubMed: 21813473]
50. Chen J, et al. Netrin-1 protects against L-Arginine-induced acute pancreatitis in mice. PLoS One. 2012; 7(9):e46201. [PubMed: 23029434]
51. Grenz A, et al. Partial netrin-1 deficiency aggravates acute kidney injury. PLoS One. 2011; 6(5):e14812. [PubMed: 21625583]
52. Han Y, et al. Netrin-1 simultaneously suppresses corneal inflammation and neovascularization. Invest Ophthalmol Vis Sci. 2012; 53(3):1285–1295. [PubMed: 22323486]
53. Mirakaj V, et al. Netrin-1 signaling dampens inflammatory peritonitis. J Immunol. 2011; 186(1): 549–555. [PubMed: 21098235]
54. Schubert T, et al. Role of the netrin system of repellent factors on synovial fibroblasts in rheumatoid arthritis and osteoarthritis. Int J Immunopathol Pharmacol. 2009; 22(3):715–722. [PubMed: 19822088]

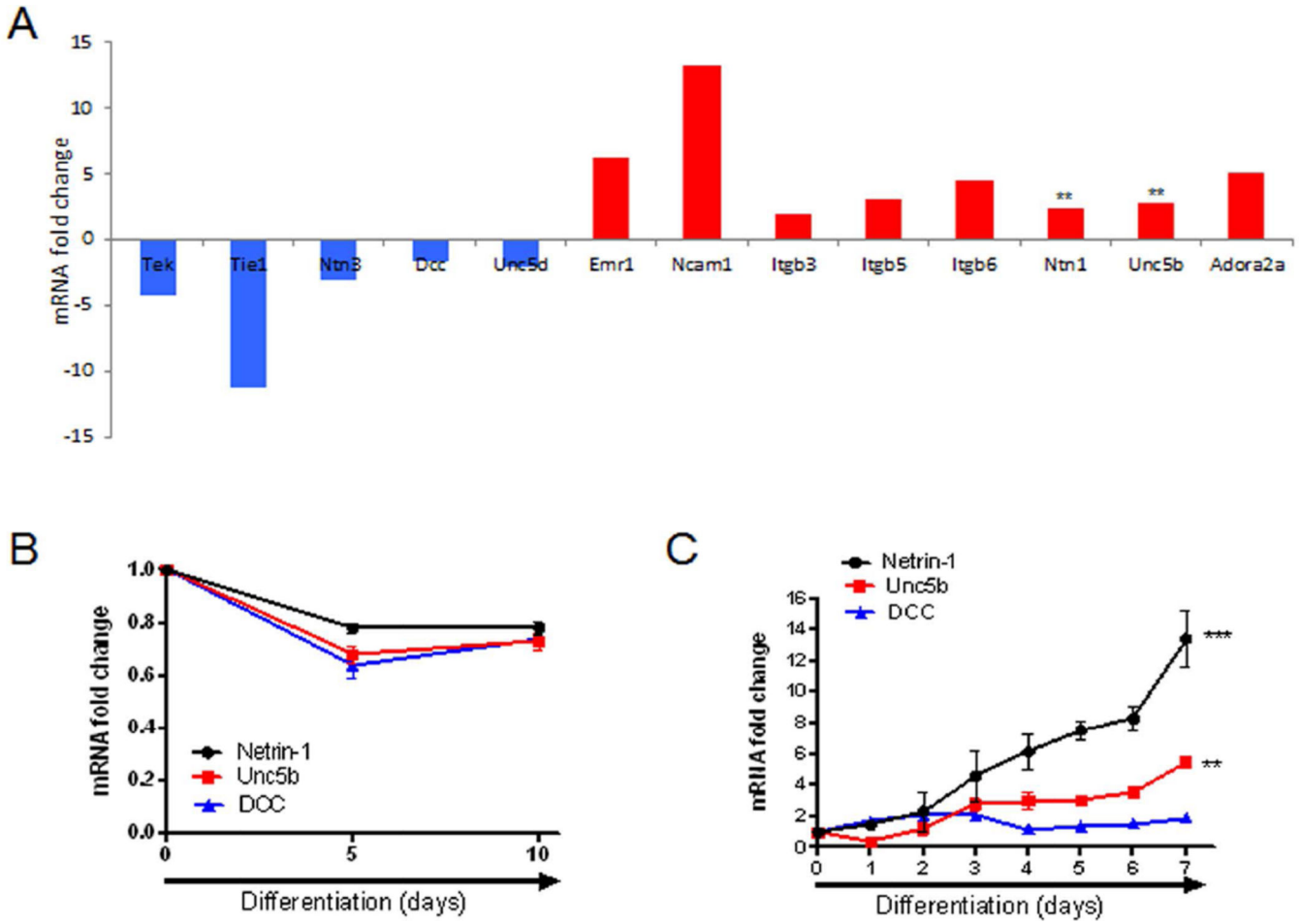

Fig. 1.

Netrin-1 and Unc5b are expressed during osteoclast but not osteoblast differentiation. (*A*) Total RNA was extracted from both undifferentiated and osteoclast-derived RAW264.7 cells, and quantitative RT-PCR analysis of the Netrin-1 guidance cue members was performed using RT2 Custom Profiler PCR Arrays. Fold change in expression is shown. (*B*) Fold change in Netrin-1, Unc5b, and DCC mRNA in osteogenic differentiated osteoblast after 10 days of osteoblast differentiaion in murine BMCs. (*C*) Fold change in Netrin-1, Unc5b, and DCC mRNA in murine M-CSF/RANKL osteoclast precursors during the 7 days of osteoclast differentiaion. ***$p < 0.001$, **$p < 0.01$, versus nonstimulated control (Student's *t* test).

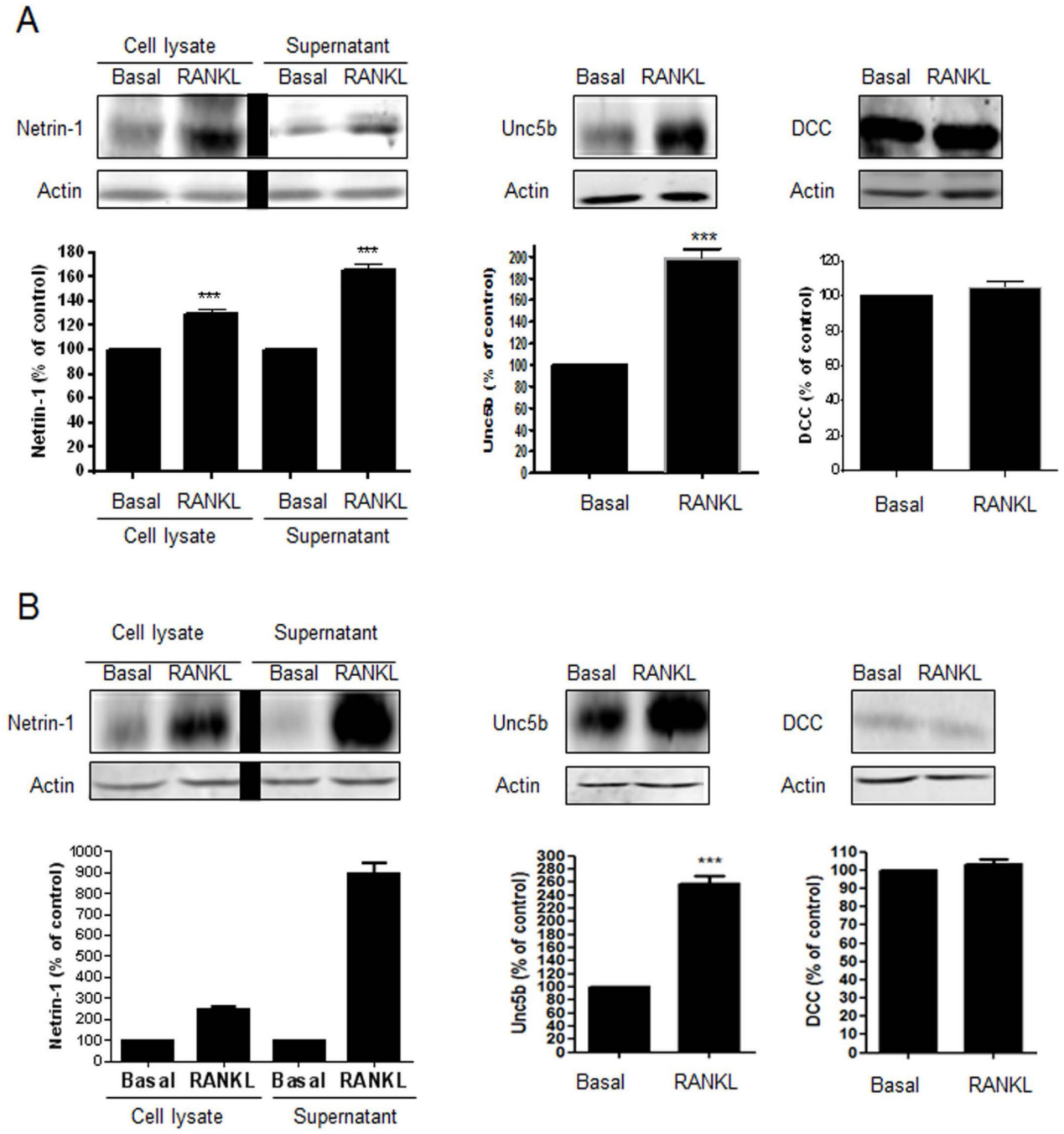

Fig. 2.

Netrin-1 and Unc5b are increased during osteoclast differentiation. (*A*) Netrin-1 expression and secretion and Unc5b and DCC expression were analyzed 24 hours after RANKL stimulation in murine BMCs cells. (*B*) Netrin-1 expression and secretion and Unc5b and DCC expression were analyzed 24 hours after RANKL stimulation in human BMCs cells. The results were expressed as the means of four independent experiments. ***$p < 0.001$, **$p < 0.01$ versus nonstimulated control (Student's *t* test or ANOVA).

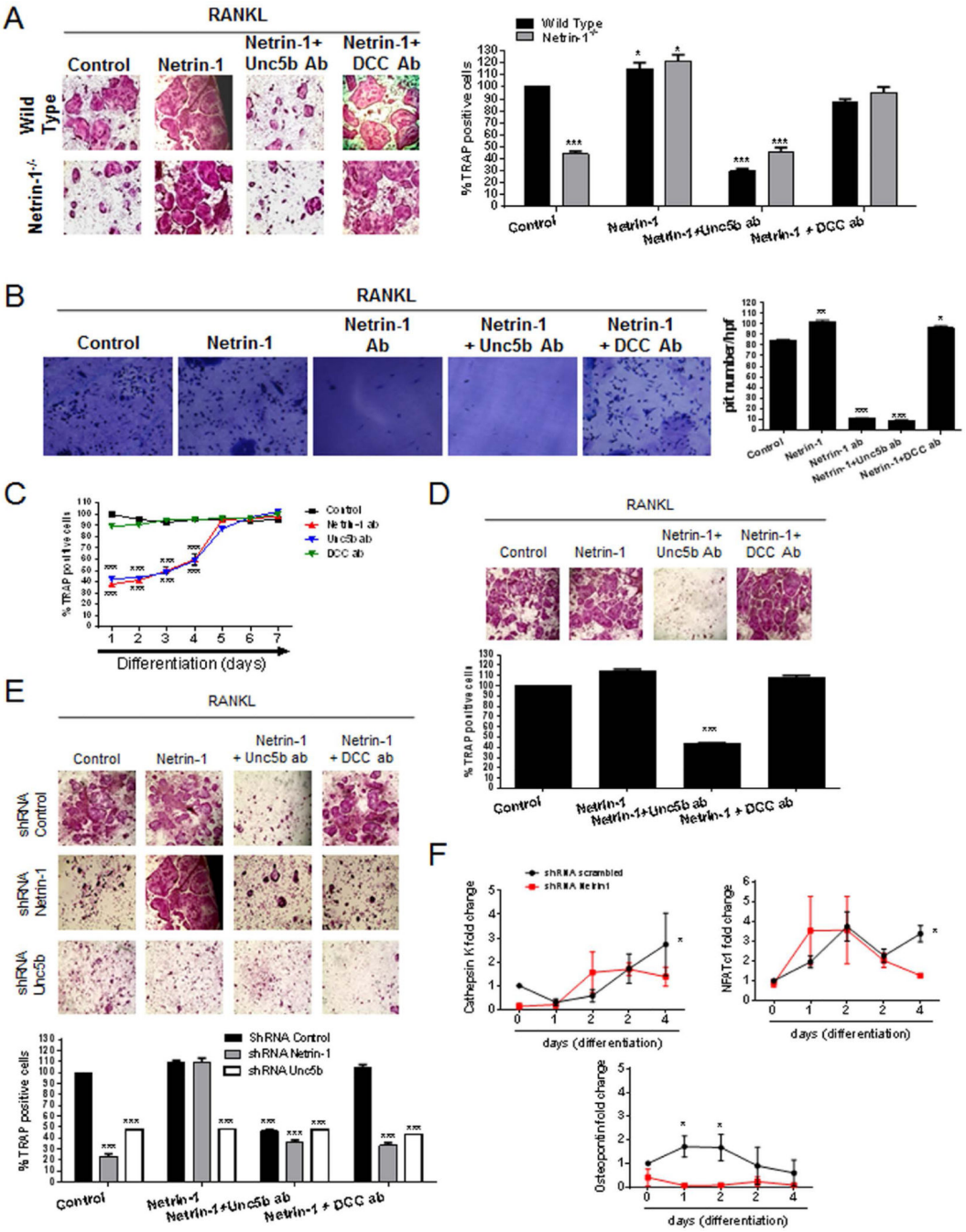

Fig. 3.

In vitro characterization of bone marrow–derived osteoclast. (*A*) WT and Netrin-1$^{-/-}$ mice osteoclast primary culture cells were fixed and stained for TRAP after being cultured for 7 days in the presence of recombinant Netrin-1 alone or combined with Unc5b or DCC antibodies. TRAP-positive cells containing three or more nuclei were counted as osteoclasts. (*B*) Toluidine blue staining to assay osteoclast activity. Nonadherent cells were seeded in dentin slides and treated for 7 days in the presence of recombinant Netrin-1 alone or combined with Unc5b or DCC antibodies. (*C*) Day response effect of Netrin-1 blockade on

osteoclast differentiation. Netrin-1, Unc5b, and DCC antibodies were exposed to cultures at various time points after the start of the cultures. WT mouse osteoclast primary culture cells stained with TRAP to counteract osteoclast. (*D*) Human primary BMC-derived osteoclast culture cells were fixed and stained for TRAP after being cultured for 7 days in the presence of recombinant Netrin-1 alone or combined with Unc5b or DCC antibodies. TRAP-positive cells containing three or more nuclei were counted as osteoclasts. (*E*) RAW264.7 cells were permanently transfected with scrambled, Netrin-1, or Unc5b shRNA, and treated with 50 ng/mL RANKL together with recombinant Netrin-1 alone or in the presence of Unc5b and DCC antibodies. Cells were fixed and stained for TRAP after being cultured for 7 days. TRAP-positive cells containing three or more nuclei were counted as osteoclasts. (*F*) RAW264.7 cells were stably transduced with scrambled or Netrin-1 shRNA and treated with 50 ng/mL RANKL. Changes in cathepsin K, NFATc1, and osteopontin mRNA during the 4-day osteoclast differentiation process in Netrin-1 shRNA RAW264.7 cells were compared with scrambled shRNA-infected cells. All data are expressed as means ± SEM of four independent cultures. ***$p < 0.001$, *$p < 0.05$ related to control (ANOVA).

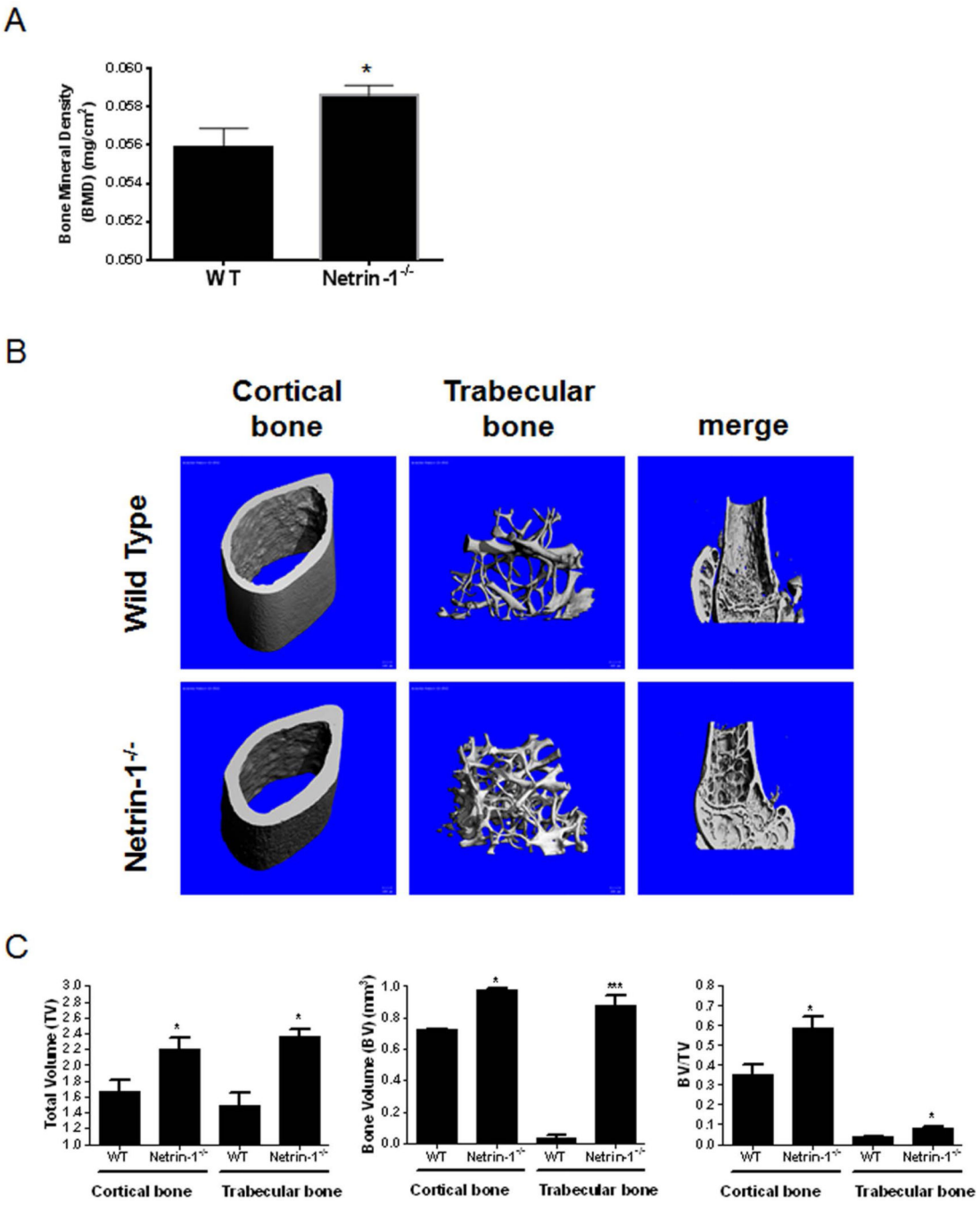

Fig. 4.

Morphometric examination of long bones in 5-month-old WT and Netrin-1$^{-/-}$mice. (*A*) Whole-body dual X-ray absorptiometry (DXA) scanning to assess the bone mineral density (BMD) (gm/cm^2) of the whole skeletons of Netrin-1$^{-/-}$ and wild-type (WT) mice (n = 9 each). (*B*) Representative high-resolution micro-CT images. Three-dimensional images of the reconstruction of the femurs revealed increased bone mass in Netrin-1$^{-/-}$ mice compared with their WT littermates (n = 5 each). (*C*) Digital morphometric analysis of micro-CT

images from WT and Netrin-$1^{+/-}$ mice. All data are expressed as means ± SEM. ***$p < 0.001$, *$p < 0.05$ related to WT (Student's *t* test or ANOVA).

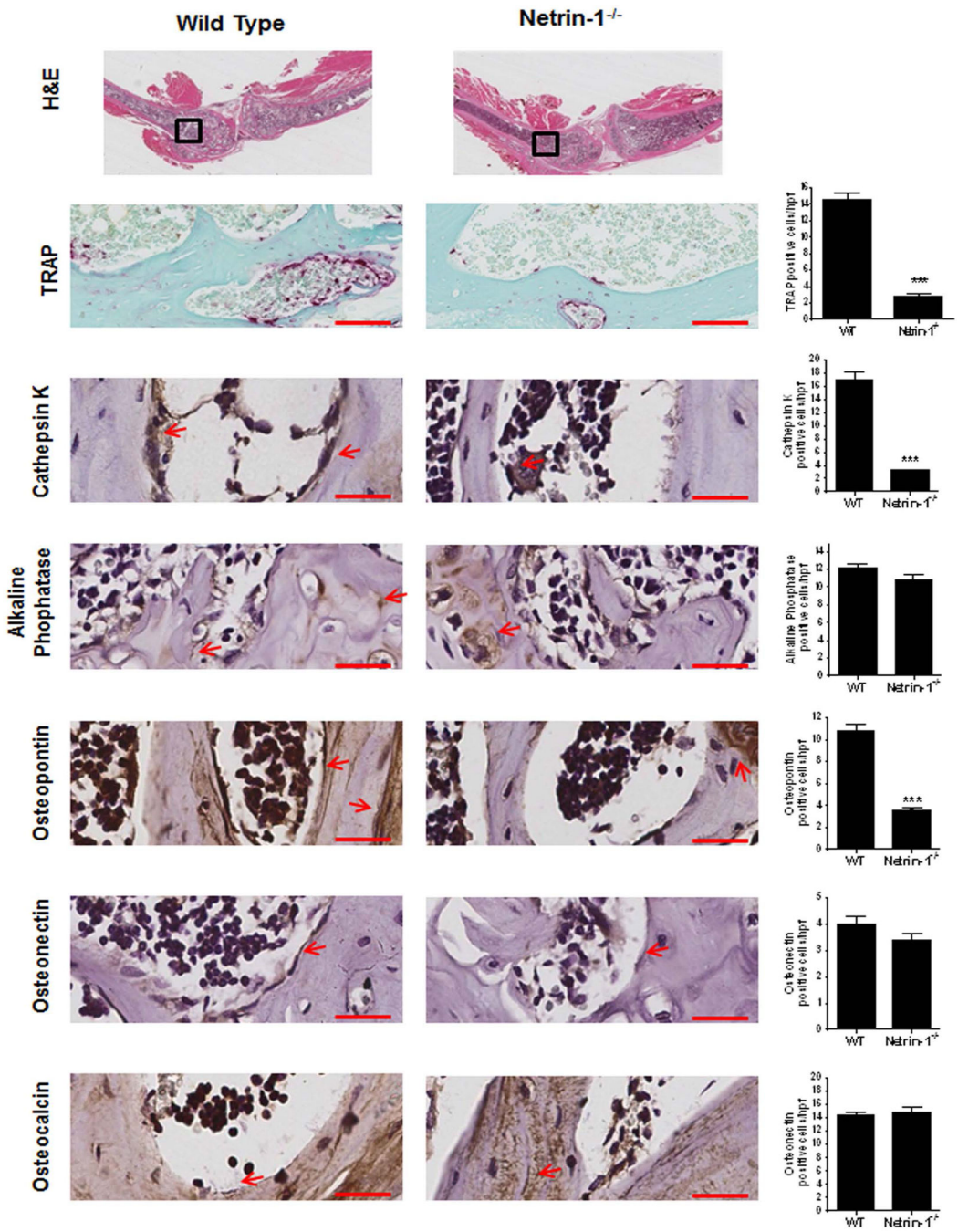

Fig. 5.

Histological examination of long bone from WT and Netrin-1$^{-/-}$ mice. Long bones (femur and tibias) were stained with hematoxylin and eosin to determine morphology. Representative histologic sections obtained from the femurs of WT and Netrin-1$^{-/-}$ mice, stained for TRAP and cathepsin K as markers of osteoclasts, alkaline phosphatase as a marker of osteoblasts. Osteopontin, osteonectin, and osteocalcin were counterstained with hematoxylin. Quantification of the number of osteoclasts/hpf (high-power field) was performed by counting positive cells in five different images for each of 3 mice. All images

are taken with the same magnification. Scale bar = 50 μm. Data represent means ± SEM (n = 3 per group) of results from slides from different mice. ***$p < 0.001$, **$p < 0.01$ related to saline (ANOVA).

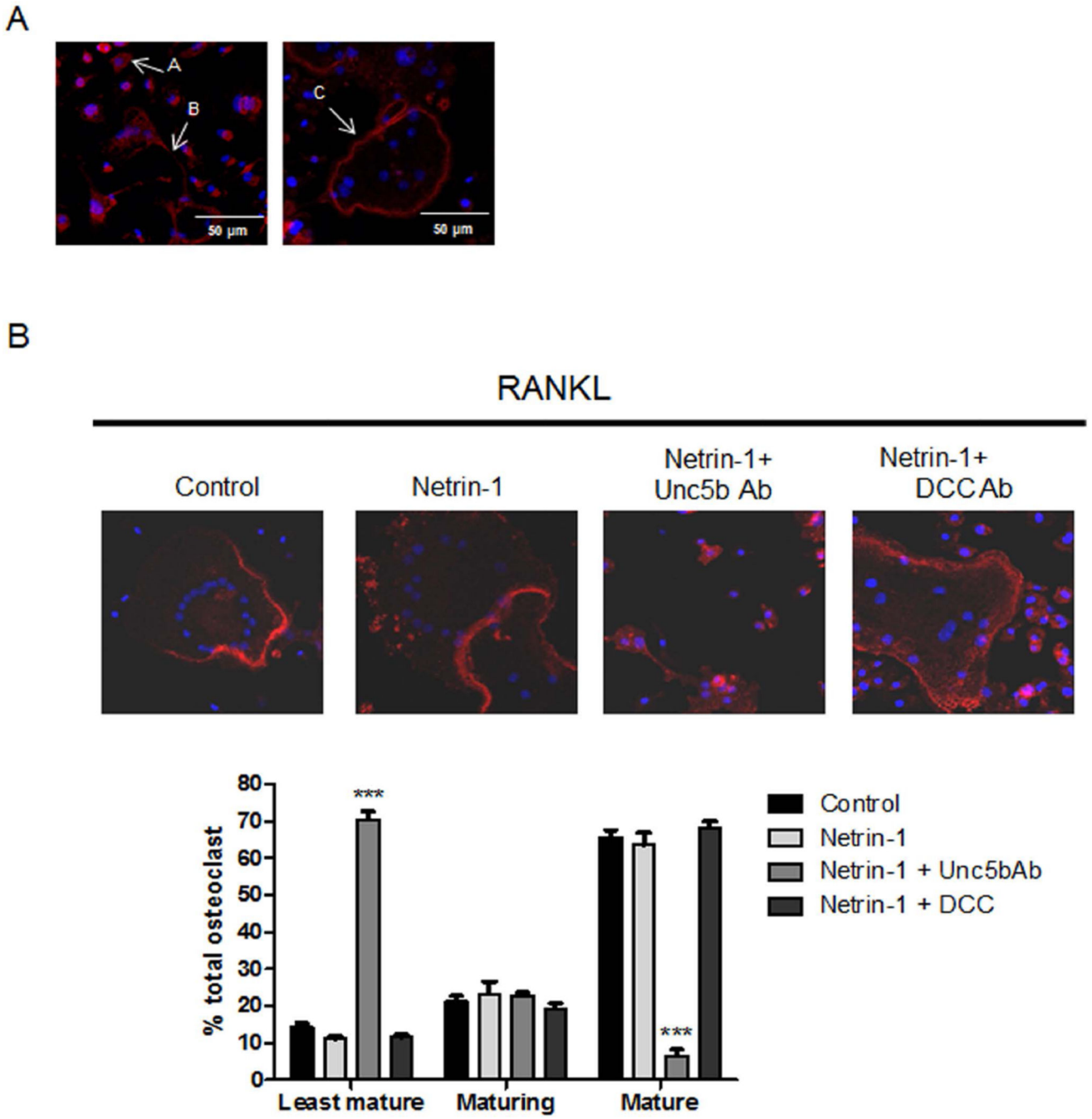

Fig. 6.

Morphological characterization of osteoclast cultures. (*A*) Morphology of the least mature (arrow A), maturing (arrow B), and mature osteoclasts (arrow C) cultured on glass. (*B*) Quantitative evaluation of number of least mature, maturing, and mature osteoclasts in osteoclast cultures treated with recombinant Netrin-1 alone or in the presence of Unc5b and DCC antibodies. F-actin was detected by Alexa 555-Phalloidin staining in osteoclast cultures treated. Images taken at ×63 magnification. The results were expressed as the means of four independent experiments.

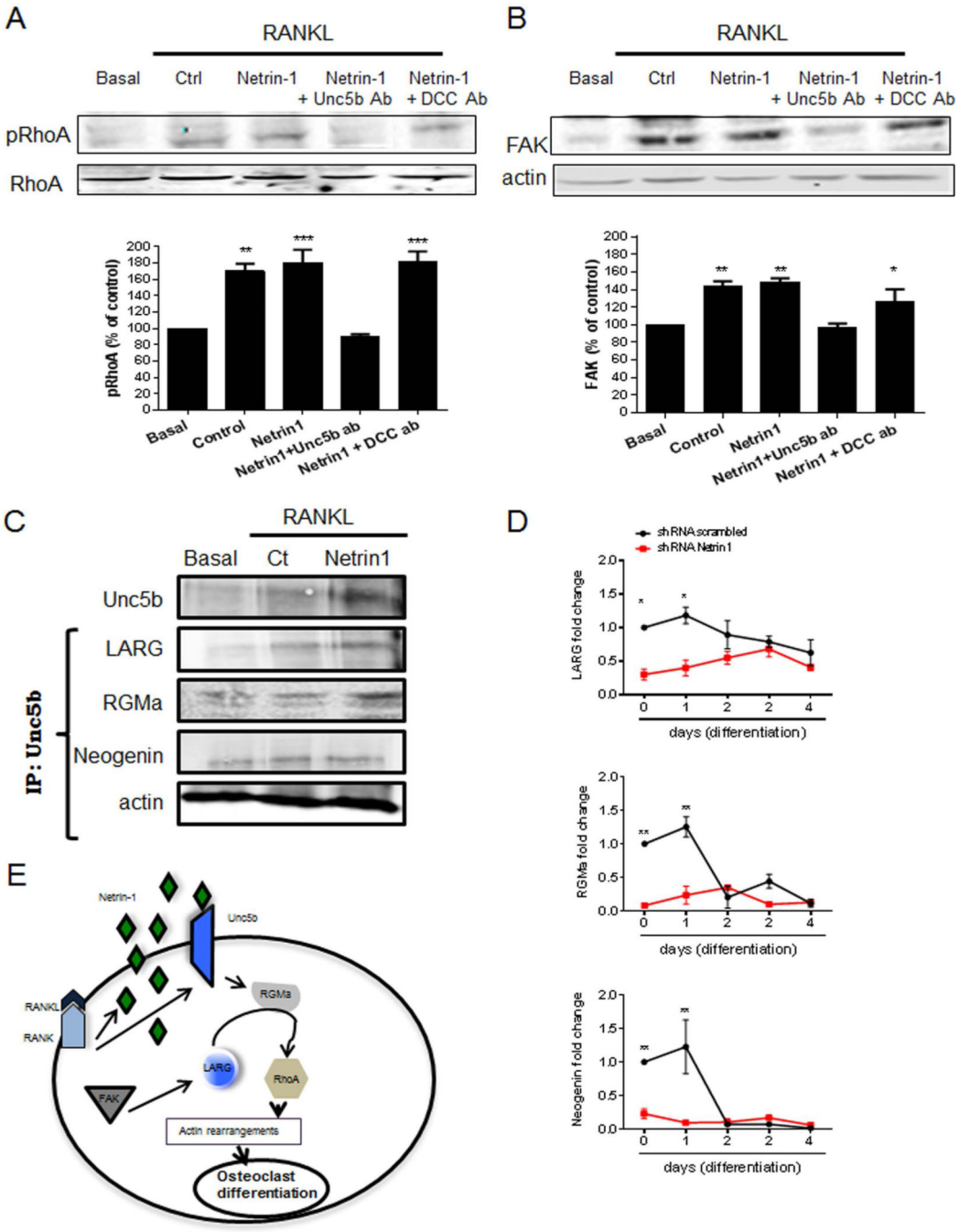

Fig. 7.

Netrin-1 and Unc5b interactions led to RhoA phosphorylation and FAK activation. Murine BMCs were treated with 30 ng/mL RANKL together with recombinant Netrin-1 alone or in combination with Unc5b or DCC antibodies. (*A*) RhoA phosphorylation was analyzed 15 minutes after stimulation by Western blot of lysates. (*B*) FAK expression was analyzed 15 minutes after stimulation by Western blot of lysates. To normalize for protein loading, the membranes were reprobed with RhoA or actin, respectively, and results normalized appropriately. (*C*) Cell extracts were immunoprecipitated with anti-Unc5b antibody. The

immunoprecipitates were then analyzed by immunoblotting with anti-Neogenin, anti-LARG, and anti-RGMa antibodies. The figure shows representative data from one of four experiments. (*D*) RAW264.7 cells were stably transduced with scrambled or Netrin-1 shRNA and treated with 50 ng/mL RANKL. Changes in LARG, RGMa, and Neogenin mRNA during the 4-day osteoclast differentiation process in Netrin-1 shRNA RAW264.7 cells were compared with scrambled shRNA-infected cells. (*E*) Proposed intracellular pathway activated by Netrin-1/Unc5b to promote changes in RhoA cytoskeleton. The results were expressed as the means of four independent experiments. ***$p < 0.001$, **$p < 0.01$, *$p < 0.5$ versus nonstimulated control.

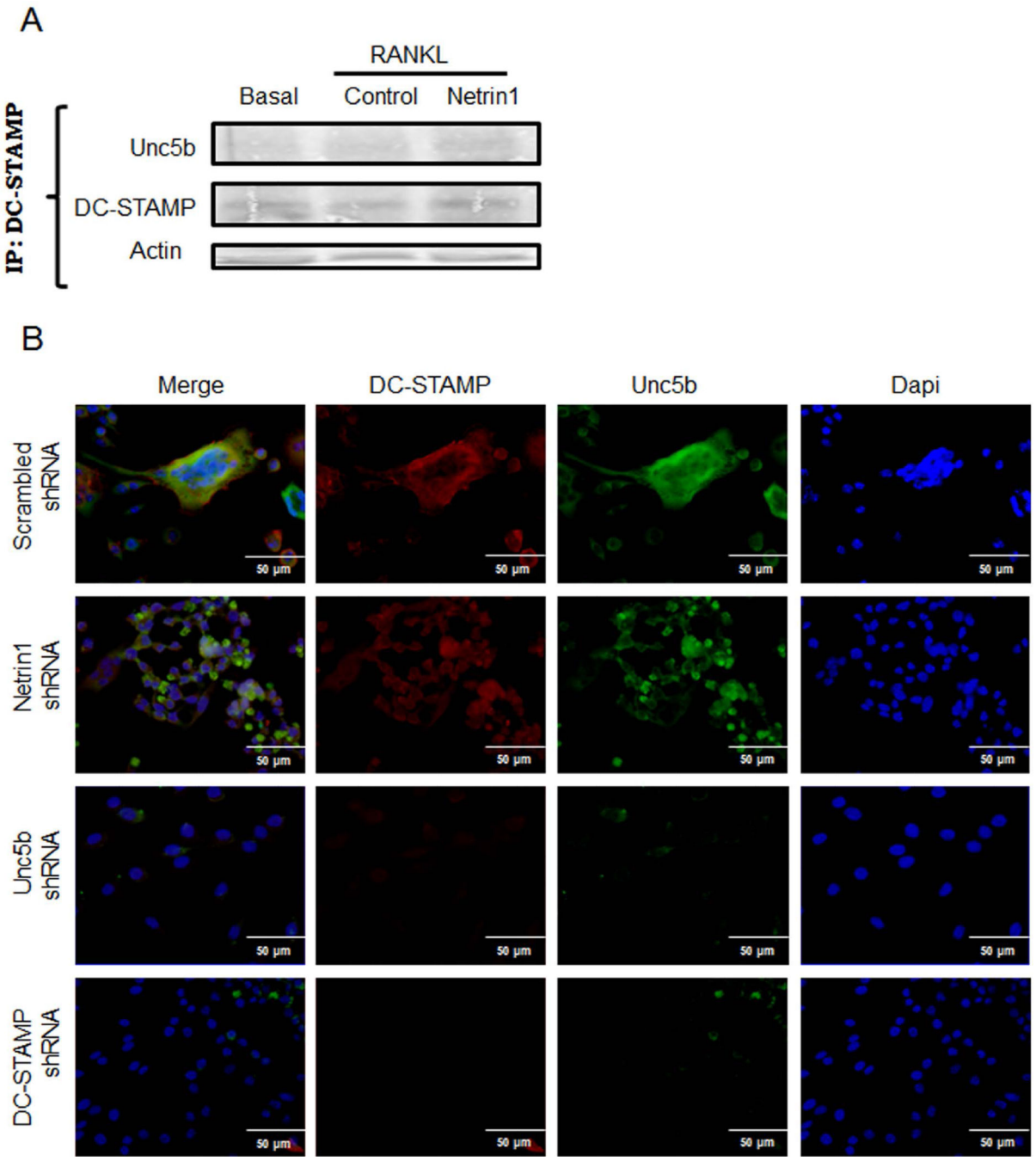

Fig. 8.

Stimulation of Unc5b promotes cell fusion associated with DC-STAMP. (*A*) Murine BMCs were treated with 30 ng/mL RANKL together with recombinant Netrin-1. Cell extracts were immunoprecipitated with anti-Unc5b antibody. The immunoprecipitates were then analyzed by immunoblotting with anti-DC-STAMP antibody. The figure shows representative data from one of four experiments. (*B*) RAW264.7 cells were stably transduced with scrambled or Netrin-1, Unc5b, or DC-STAMP shRNA and treated with 50 ng/mL RANKL for 4 days.

DC-STAMP immunostaining is shown in green and Unc5b immunolocalization is shown in red. Images were taken at an original magnification of ×63.

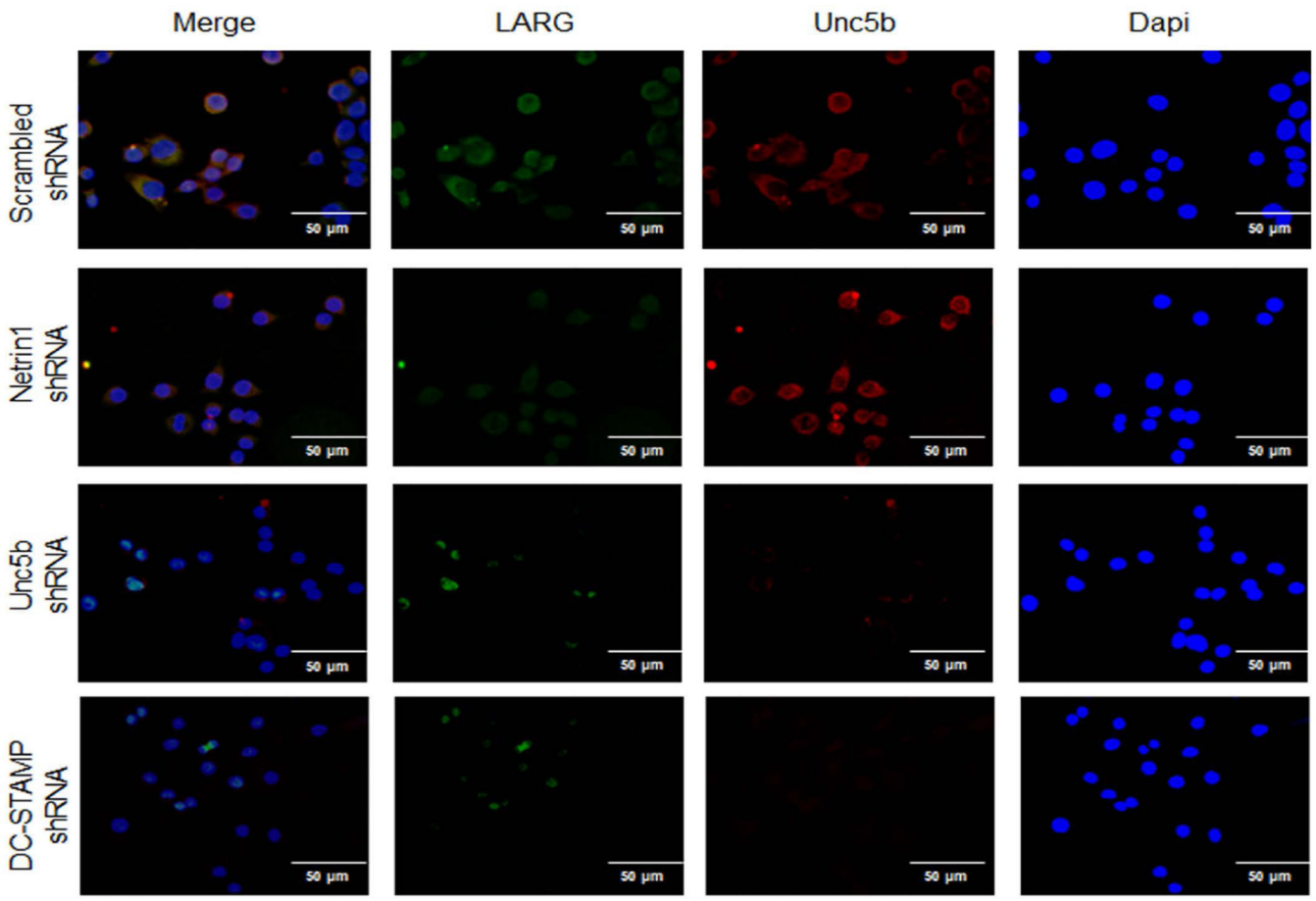

Fig. 9.

Unc5b modulates the expression of LARG in osteoclast precursors. RAW264.7 cells were stably transduced with scrambled or Netrin-1, Unc5b, or DC-STAMP shRNA and treated with 50 ng/mL RANKL for 24 hours. LARG immunostaining is shown in green and Unc5b immunolocalization is shown in red. Images were taken at an original magnification of ×63.

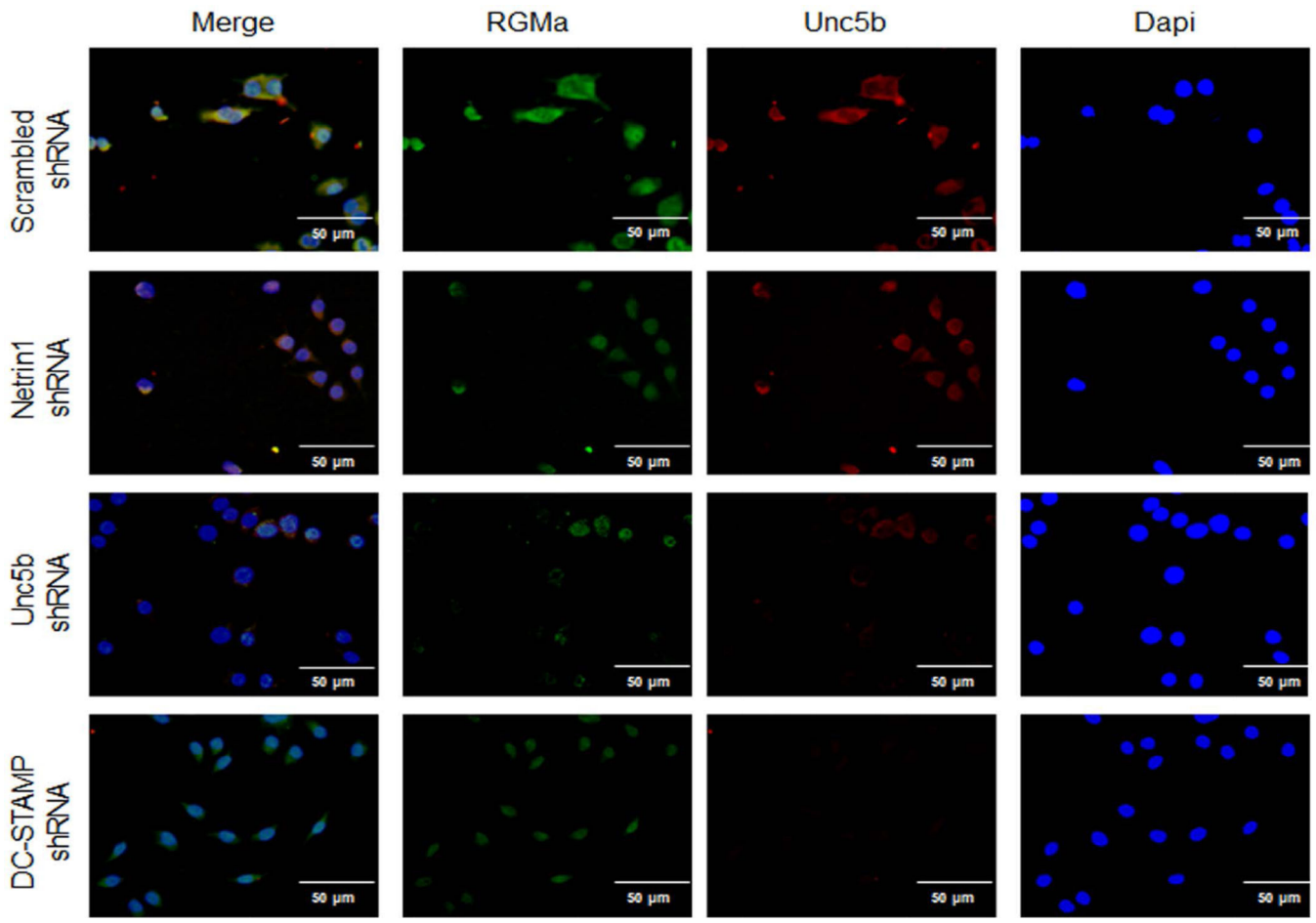

Fig. 10.

Unc5b modulates the expression of RGMa in osteoclast precursors. RAW264.7 cells were stably transduced with scrambled or Netrin-1, Unc5b, or DC-STAMP shRNA and treated with 50 ng/mL RANKL for 24 hours. RGMa immunostaining is shown in green and Unc5b immunolocalization is shown in red. Images were taken at an original magnification of ×63.

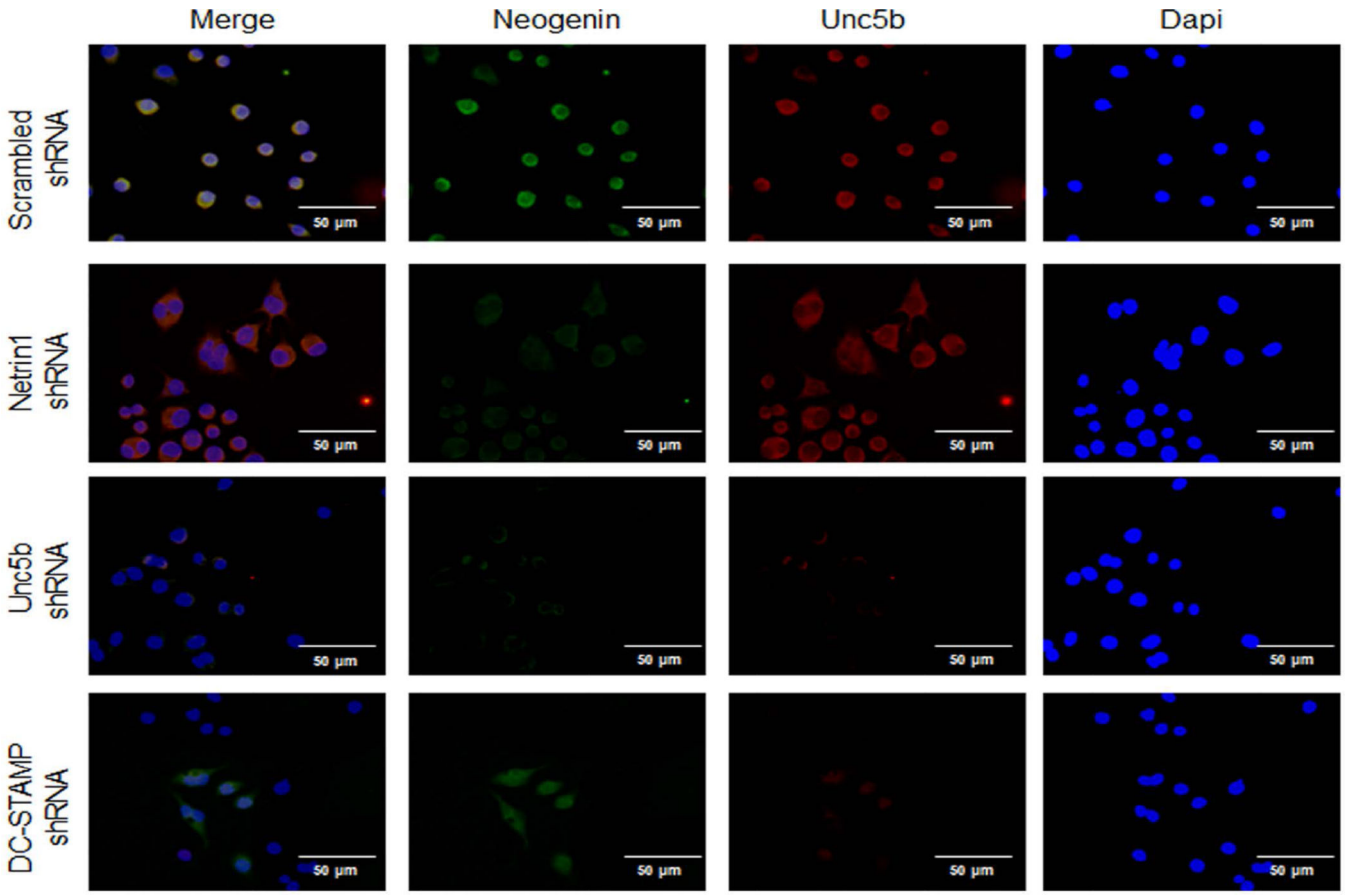

Fig. 11.

Unc5b modulates the expression of Neogenin in osteoclast precursors. RAW264.7 cells were stably transduced with scrambled or Netrin-1, Unc5b, or DC-STAMP shRNA and treated with 50 ng/mL RANKL for 24 hours. Neogenin immunostaining is shown in green and Unc5b immunolocalization is shown in red. Images were taken at an original magnification of ×63.

Table 1

Histomorphometric Measures of Long Bones in 5-Month-Old WT and Netrin-$1^{-/-}$ Mice

	Wild type	Netrin-$1^{-/-}$
Bone volume (BV, mm^3)	72.61 ± 2.09	85.67 ± 1.57***
Trabecular volume (TV, %)	75.70 ± 2.05	85.60 ± 1.63***
BV/TV	0.87 ± 0.04	0.94 ± 0.05*
Trabecular number (Tb.N)	0.28 ± 0.04	0.63 ± 0.02***
Trabecular separation (Tb.Sp, μm)	327.47 ± 8.30	341.15 ± 7.06*
Osteoid number	6.53 ± 0.91	9.51 ± 1.82*
Osteoid surface (OS/BS)	0.32 ± 0.10	0.42 ± 0.07*
Osteoblast number (Ob.N)	22.4 ± 4.65	29.5 ± 2.10*
Osteoblast surface (Ob.N/BS)	0.35 ± 0.09	0.39 ± 0.02*
Osteoclast number (Oc.N)	28.75 ± 4.10	19.00 ± 3.51*
Osteoclast surface (Oc.S)	0.51± 0.16	0.36 ± 0.02*

Histomorphometric measures on long bones were calculated using the Bioquant Osteo software (mean ± SEM, $n = 4$ per group).

*** $p < 0.001$,

* $p < 0.05$ versus wild type (Student's t test).